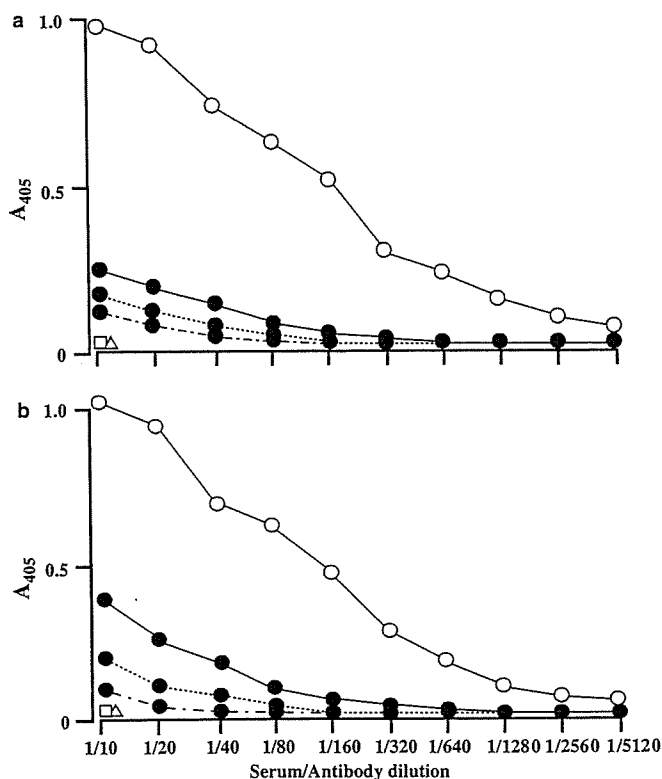


**Fig. 5a,b** Morphological effects of repeated administration of yr-haGal on renal tubular cells of Fabry mice. yr-haGal was repeatedly injected into Fabry mice; kidney tissues were then examined by electron microscopy. **a** An untreated Fabry mouse.

**b** A Fabry mouse treated with yr-haGal. Many lamellar inclusion bodies can be seen in the renal tubular cells of the untreated Fabry mice, and the number of lamellar inclusion bodies is apparently decreased after repeated administration of yr-haGal. Bar 2  $\mu$ m

In conclusion, we produced in yeast cells a recombinant  $\alpha$ -galactosidase with M6P residues at the non-reducing ends of *N*-linked sugar chains. This recombinant enzyme was incorporated into the liver, kidneys, heart and spleen, and degraded the accumu-

lated CTH in these tissues, although cleavage of the CTH accumulated in the dorsal root ganglia was insufficient. As production of recombinant  $\alpha$ -galactosidase in yeast is easy and economical, and does not require fetal calf serum, yr-haGal is highly promising as an enzyme source for enzyme replacement therapy for Fabry disease.



**Fig. 6** Antigenicity of yr-haGal and agalsidase beta. ELISA was performed to determine whether Fabry mice recurrently injected with yr-haGal (**a**) or agalsidase beta (**b**) produced antibodies to the enzymes or not. *Open circles* Rabbit anti- $\alpha$ -galactosidase antibodies, *closed circles* Fabry mouse sera treated with the enzymes (yr-haGal and agalsidase beta), *open squares* serum from an untreated Fabry mouse, *open triangles* serum from an untreated wild type mouse

**Acknowledgements** We wish to thank Drs. Ashok B. Kulkarni (Gene Targeting Facility and Functional Genomics Unit, NIDCR, NIH) and Toshio Ohshima (Laboratory for Developmental Neurology, Brain Science Institute, RIKEN), and also Drs. Ryoichi Kase, Fumiko Matsuzawa and Sei-ichi Aikawa (The Tokyo Metropolitan Institute of Medical Science) for their technical support. This work was partly supported by grants from the Tokyo Metropolitan Government, the Japan Society for the Promotion of Science, the Ministry of Education, Science, Sports and Culture, and the Ministry of Health, Labor and Welfare of Japan.

## References

- Chiba Y, Suzuki M, Yoshida S, Yoshida A, Ikenaga H, Takeuchi M, Jigami Y, Ichishima E (1998) Production of human compatible high mannose-type ( $\text{Man}_5\text{GlcNAc}_2$ ) sugar chains in *Saccharomyces cerevisiae*. *J Biol Chem* 273:26298-26304
- Chiba Y, Sakuraba H, Kotani M, Kase R, Kobayashi K, Takeuchi M, Ogasawara S, Maruyama Y, Nakajima T, Takaoka Y, Jigami Y (2002) Production in yeast of  $\alpha$ -galactosidase A, a lysosomal enzyme applicable to enzyme replacement therapy for Fabry disease. *Glycobiology* 12:821-828
- Desnick RJ, Ioannou YA, Eng CM (2001)  $\alpha$ -Galactosidase A deficiency: Fabry disease. In: Scriver CR, Beaudet AL, Sly WS, Valle D (eds) *The metabolic and molecular bases of inherited disease*, 8th edn. McGraw-Hill, New York, pp 3733-3774
- Desnick RJ, Brady RO, Barranger J, Collins AJ, Germain DP, Goldman M, Grabowski G, Packman S, Wilcox WR (2003) Fabry disease, an under-recognized multisystemic disorder: expert recommendations for diagnosis, management, and enzyme replacement therapy. *Ann Intern Med* 138:338-346
- Eng CM, Banikzemi M, Gordon RE, Goldman M, Phelps R, Kim L, Gass A, Winston J, Dikman S, Fallon JT, Brodie S, Stacy CB, Mehta D, Parsons R, Norton K, O'Callaghan M, Desnick RJ (2001a) A phase 1/2 clinical trial of enzyme replacement in Fabry disease: pharmacokinetic, substrate clearance, and safety studies. *Am J Hum Genet* 68:711-722

- Eng CM, Guffon N, Wilcox WR, Germain DP, Lee P, Waldek S, Caplan L, Linthorst GE, Desnick RJ (2001b) Safety and efficacy of recombinant human  $\alpha$ -galactosidase A replacement therapy in Fabry's disease. *N Engl J Med* 345:9-16
- Fukushima M, Tsuchiyama Y, Nakato T, Yokoi T, Ikeda H, Yoshida S, Kusumoto T, Itoh K, Sakuraba H (1995) A female heterozygous patient with Fabry's disease with renal accumulation of trihexosylceramide detected with a monoclonal antibody. *Am J Kidney Dis* 26:952-955
- Ishii S, Kase R, Sakuraba H, Fujita S, Sugimoto M, Tomita K, Semba T, Suzuki Y (1994) Human  $\alpha$ -galactosidase gene expression: significance of two peptide regions encoded by exons 1-2 and 6. *Biochim Biophys Acta* 1204:265-270
- Itoh K, Kotani M, Tai T, Suzuki H, Utsunomiya T, Inoue H, Yamada H, Sakuraba H, Suzuki Y (1993) Immunofluorescence imaging diagnosis of Fabry heterozygotes using confocal laser scanning microscopy. *Clin Genet* 44:302-306
- Itoh K, Takenaka T, Nakao S, Setoguchi M, Tanaka H, Suzuki T, Sakuraba H (1996) Immunofluorescence analysis of globotriaosylceramide accumulated in the hearts of variant hemizygotes and heterozygotes with Fabry disease. *Am J Cardiol* 78:116-117
- Kornfeld S, Sly WS (2001) I-cell disease and pseudo-Hurler polydystrophy: disorders of lysosomal enzyme phosphorylation and localization. In: Scriver CR, Beaudet AL, Sly WS, Valle D (eds) *The metabolic and molecular bases of inherited disease*, 8th edn. McGraw-Hill, New York, pp 3469-3482
- Kotani M, Kawashima I, Ozawa H, Ogura K, Ariga T, Tai T (1994) Generation of one set of murine monoclonal antibodies specific for globo-series glycolipids: evidence for differential distribution of the glycolipids in rat small intestine. *Arch Biochem Biophys* 310:89-96
- Kotani M, Yamada H, Sakuraba H (2004) Cytochemical and biochemical detection of intracellularly accumulated sialyl glycoconjugates in sialidosis and galactosialidosis fibroblasts with *Maakia amurensis*. *Clin Chim Acta* 344:131-135
- Lee K, Jin X, Zhang K, Copertino L, Andrews L, Baker-Malcolm J, Geagen L, Qui H, Seiger K, Barngrover D, McPherson JM, Edmunds T (2003) A biochemical and pharmacological comparison of enzyme replacement therapies for the glycolipid storage disorder Fabry disease. *Glycobiology* 13:305-313
- Lyon MF (1962) Sex chromatin and gene action in the mammalian X-chromosome. *Am J Hum Genet* 14:135-148
- Mehta A, Ricci R, Widmer U, Dehout F, Garcia de Lorenzo A, Kampmann C, Linhart A, Sunder-Plassmann G, Ries M, Beck M (2004) Fabry disease defined: baseline clinical manifestations of 366 patients in the Fabry Outcome Survey. *Eur J Clin Invest* 34:236-242
- Mayer JS, Scheerer JB, Sifers RN, Donaldson ML (1981) Differential assay for lysosomal  $\alpha$ -galactosidase in human tissues and its application to Fabry's disease. *Clin Chim Acta* 112:247-251
- Nakao S, Takenaka T, Maeda M, Kodama C, Tanaka A, Tahara M, Yoshida A, Kuriyama M, Hayashibe H, Sakuraba H, Tanaka H (1995) An atypical variant of Fabry's disease in men with left ventricular hypertrophy. *N Engl J Med* 333:288-293
- Odani T, Shimma Y, Tanaka A, Jigami Y (1996) Cloning and analysis of the *MNN4* gene required for phosphorylation of *N*-linked oligosaccharides in *Saccharomyces cerevisiae*. *Glycobiology* 6:805-810
- Ohsawa M, Kotani M, Tajima Y, Tsuji D, Ishibashi Y, Kuroki A, Itoh K, Watabe K, Sango K, Yamanaka S, Sakuraba H (2005) Establishment of immortalized Schwann cells from Sandhoff mice and corrective effect of recombinant human  $\beta$ -hexosaminidase A on the accumulated GM2 ganglioside. *J Hum Genet* 50:460-467
- Rosenfeld EL, Belenky DM, Bystrov NK (1986) Interaction of hepatic asialoglycoprotein receptor with asialoorosomucoid and galactolyzed lysosomal  $\alpha$ -glucosidase. *Biochim Biophys Acta* 883:306-312
- Sakuraba H, Yanagawa Y, Igarashi T, Suzuki Y, Suzuki T, Watanabe K, Ieki K, Shimoda K, Yamanaka T (1986) Cardiovascular manifestations in Fabry's disease. A high incidence of mitral valve prolapse in hemizygotes and heterozygote. *Clin Genet* 29:276-283
- Sakuraba H, Oshima A, Fukuhara Y, Shimamoto M, Nagao Y, Bishop DF, Desnick RJ, Suzuki Y (1990) Identification of point mutations in the  $\alpha$ -galactosidase A gene in classical and atypical hemizygotes with Fabry disease. *Am J Hum Genet* 47:784-789
- Schiffmann R, Murray GJ, Treco D, Daniel P, Sellos-Moura M, Myers M, Quirk JM, Zirzow GC, Borowski M, Loveday K, Anderson T, Gillespie F, Cliver KL, Jeffries NO, Doo E, Liang TJ, Kreps C, Gunter K, Frei K, Crutchfield K, Selden RF, Brady RO (2000) Infusion of  $\alpha$ -galactosidase A reduces tissue globotriaosylceramide storage in patients with Fabry disease. *Proc Natl Acad Sci USA* 97:365-370
- Takahashi H, Hirai Y, Migita M, Seino Y, Fukuda Y, Sakuraba H, Kase R, Kobayashi T, Hashimoto Y, Shimada T (2002) Long-term systemic therapy of Fabry disease in a knockout mouse by adeno-associated virus-mediated muscle-directed gene transfer. *Proc Natl Acad Sci USA* 99:13777-13782
- Takashiba M, Chiba Y, Arai E, Jigami Y (2004) Analysis of mannose-6-phosphate labeled with 8-aminopyrene-1,3,6-trisulfonate by capillary electrophoresis. *Anal Biochem* 332:196-198
- Thurnberg BL, Rennke H, Colvin RB, Dikman S, Gordon RE, Collins AB, Desnick RJ, O'Callaghan M (2002) Globotriaosylceramide accumulation in the Fabry kidney is cleared from multiple cell types after enzyme replacement therapy. *Kidney Int* 62:1933-1946

# Sox10 regulates ciliary neurotrophic factor gene expression in Schwann cells

Yasuhiro Ito\*, Stefan Wiese\*, Natalja Funk\*, Alexandra Chittka\*, Wilfried Rossoll\*, Heike Bömmel\*, Kazuhiko Watabe†, Michael Wegner‡, and Michael Sendtner\*<sup>§</sup>

\*Institute for Clinical Neurobiology, University of Wuerzburg, D-97080 Wuerzburg, Germany; †Department of Molecular Neuropathology, Tokyo Metropolitan Institute for Neuroscience, 2-6 Musashidai, Fuchu-shi, Tokyo 183-8526, Japan; and ‡Institute of Biochemistry, Erlangen University, D-91054 Erlangen, Germany

Communicated by Hans Thoenen, Max Planck Institute of Neurobiology, Martinsried, Germany, March 29, 2006 (received for review November 16, 2005)

Ciliary neurotrophic factor (*Cntf*) plays an essential role in postnatal maintenance of spinal motoneurons. Whereas the expression of this neurotrophic factor is low during embryonic development, it is highly up-regulated after birth in myelinating Schwann cells of rodents. To characterize the underlying transcriptional mechanisms, we have analyzed and compared the effects of various glial transcription factors. In contrast to Pit-1, Oct-1, Unc-86 homology region (POU) domain class 3, transcription factor 1 (Oct6/SCIP/Tst-1) and paired box gene 3 (*Pax3*), SRY-box-containing gene 10 (*Sox10*) induces *Cntf* expression in Schwann cells. Subsequent promoter analysis using luciferase reporter gene and EMSA identified the corresponding response elements within the *Cntf* promoter. Overexpression of *Sox10* in primary sciatic nerve Schwann cells leads to a >100-fold up-regulation of *Cntf* protein, and suppression of *Sox10* by RNA interference in the spontaneously immortalized Schwann cell line 32 reduces *Cntf* expression by >80%. Mice with heterozygous inactivation of the *Sox10* gene show significantly reduced *Cntf* protein levels in sciatic nerves, indicating that *Sox10* is necessary and sufficient for regulating *Cntf* expression in the peripheral nervous system.

promoter | Hirschsprung disease | Oct6 | neuropathy | *Pax3*

Schwann cells play an important role for maintenance of motoneurons. Their development is regulated by various transcription factors (1), including paired box gene 3 (*Pax3*) (2), Pit-1, Oct-1, Unc-86 homology region (POU) domain class 3, transcription factor 1 (Oct-6/SCIP/Tst-1) (3–6), and SRY-box-containing gene 10 (*Sox10*) (7, 8). *Ciliary neurotrophic factor* (*Cntf*) belongs to a family of neurotrophic cytokines that promote neuronal survival (9–13) and peripheral nerve regeneration (14–16). Targeted inactivation of the *Cntf* gene in mice revealed its role in postnatal maintenance of motoneurons (17, 18). Moreover, endogenous *Cntf* modulates onset and severity of disease in patients and mouse models for motoneuron disease and other neurological disorders (19–21). In progressive motor neuronopathy and wobbler mice, *Cntf* treatment protects motoneurons from cell death and improves motor performance (22, 23), indicating that this factor is a major mediator of the protective effects of Schwann cells, both under physiological and pathological conditions.

Myelinating Schwann cells in the peripheral nervous system are the richest source of *Cntf* in adult mammals (9, 10, 24). Expression of *Cntf* in the peripheral nervous system rises at the end of the first postnatal week. The control mechanisms that regulate and restrict *Cntf* expression to myelinating Schwann cells are still not known. To analyze the regulation of *Cntf* expression, we have cloned a 4.7-kb fragment containing the complete 5' region of the murine *Cntf* gene up to the neighboring zinc finger protein (*Zfp*) gene. Using deletion and mutation analysis, we found that *Cntf* gene expression is controlled by several glial transcriptional factors. *Sox10* was identified as a key regulator of *Cntf* expression. *Sox10* overexpression in cultured primary Schwann cells leads to a >100-fold up-regulation of *Cntf*

protein levels. In addition, *Cntf* levels are significantly lower in sciatic nerves of *Sox10*<sup>+/-</sup> mice, indicating that *Sox10* acts as a major physiological regulator of *Cntf* gene expression *in vivo*.

## Results

**Reduced *Cntf* Expression in *Sox10*<sup>+/-</sup> Mice.** In comparison to other Schwann cell-specific transcription factors, *Sox10* expression is most closely linked to *Cntf* up-regulation during postnatal development (8). We therefore analyzed *Cntf* expression in *Sox10*<sup>+/-</sup> mutant mice (8). Mice with homozygous mutation of the *Sox10* gene already start to die around embryonic day 13.5 (25, 26). *Sox10* expression increases from postnatal day (P)1 to P3, whereas a strong increase of *Cntf* expression was first detectable at P7 (Fig. 1A). *Cntf* protein levels are reduced by >50% (Fig. 1B and C) in *Sox10*<sup>+/-</sup> mice.

To get more insight into the physiological relevance of this finding, we overexpressed *Sox10* in primary Schwann cells from P4 rat sciatic nerves. This treatment resulted in a >100-fold induction of *Cntf* protein levels (Fig. 1D and E). Thus, *Sox10* appears sufficient for up-regulating *Cntf* expression in early postnatal Schwann cells. We then investigated the expression of *Cntf* in the spontaneously immortalized Schwann cell line 32 (IMS32) (27). In contrast to primary Schwann cells, this cell line expresses constitutively relatively high levels of *Cntf* (Fig. 1G) and therefore was used for this experiment. Suppression of *Sox10* by RNA interference leads to significant reduction ( $P < 0.001$ ) of *Cntf* expression (Fig. 1F).

**Characterization of the Regulatory Elements and Transcription Initiation Sites Within the *Cntf* Promoter.** To characterize the *Cntf* promoter region, we cloned a 6.5-kb DNA fragment containing the complete *Cntf* gene including the 4.7-kb 5' flanking region up to *Zfp*, the neighboring gene (28). The stop codon of *Zfp* was located at -4,647 bp from the start codon of *Cntf*. We performed 3' RACE to identify the poly(A) signal for *Zfp* and found a canonical AATAAA site located at -4,549 bp from the *Cntf* ATG start codon. Because the *Cntf* promoter sequence does not contain a TATA box (29), we carried out 5' RACE. For human and rat *Cntf*, only one initiation site has been identified so far (29). We found three additional initiation sites (-10, -32, -68, and -74 bp from the ATG start codon) for mouse *Cntf* (see Fig. 5, which is published as supporting information on the PNAS web site). Five, four, six, and one clone of 16 analyzed were identified for these four transcription start sites, respectively. In addition, using sequence analysis, we identified several potential

Conflict of interest statement: No conflicts declared.

Abbreviations: *Cntf*, ciliary neurotrophic factor; IMS32, immortalized Schwann cell line 32; S1, S2, and S3, *Sox10* high mobility group type DNA-binding motifs 1, 2, and 3; S1m, S2m, and S3m, mutated S1, S2, and S3; Pn, postnatal day n.

§To whom correspondence should be addressed at: Institute for Clinical Neurobiology, Josef-Schneider-Strasse 11, University of Wuerzburg, D-97080 Wuerzburg, Germany. E-mail: sendtner@mail.uni-wuerzburg.de.

© 2006 by The National Academy of Sciences of the USA

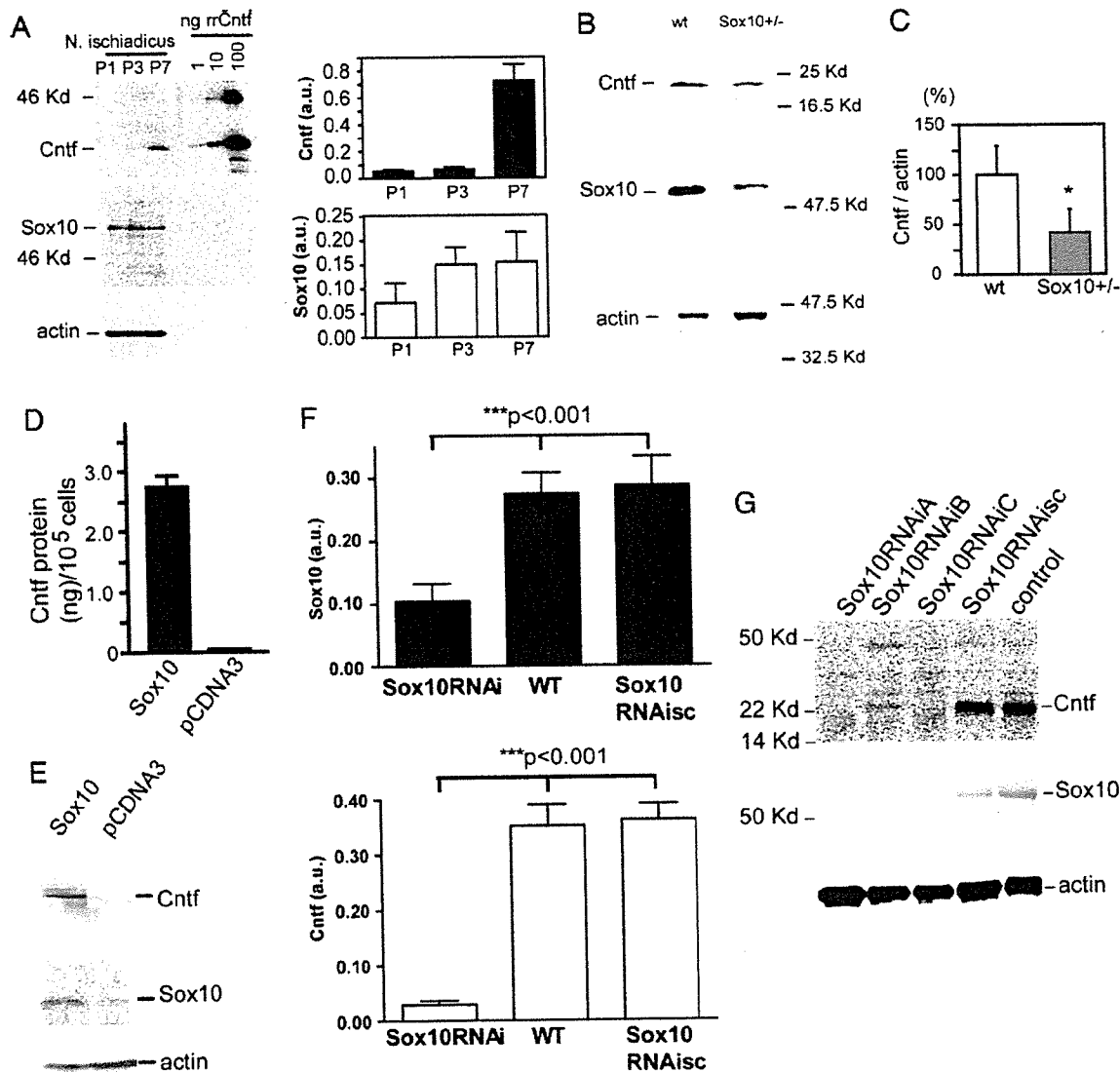


**Fig. 1.** Expression of Sox10 and Cntf in sciatic nerve of wild-type and *Sox10*<sup>+/-</sup> mutant mice. (A *Left*) Western blot analysis of sciatic nerve (*nervus ischiadicus*) extracts from P1, P3, and P7 wild-type mice. Western blots were probed for Sox10 and Cntf and reprobbed against actin as a control for equal loading. rrCntf, recombinant rat Cntf. (A *Right*) Semiquantitative analysis of Cntf and Sox10 expression from three independent experiments. Error bars represent SD. (B) Western blot analysis of sciatic nerve extracts from adult wild-type and *Sox10*<sup>+/-</sup> mice. Cntf protein was detected as one band at 22 kDa. Sox10 protein content is reduced in sciatic nerve extract of *Sox10*<sup>+/-</sup> mice. (C) The density of the Cntf immunoreactive bands was measured in three independent blots. Signals were normalized against the actin signal and are shown as percentage of wild-type levels. Error bars represent SD. \*, *P* < 0.05. (D) Cntf expression is elevated in primary Schwann cells after transient transfection of Sox10. Expression levels were estimated by measuring signal density from Western blots. A representative example is shown in C. Expression levels (mean ± SD) were quantified by using the AIDA software program. (E) Cntf expression in primary rat Schwann cells after transfection of Sox10. (F) Cntf expression is reduced after transfection of Sox10 RNA interference (RNAi) into the IMS32 Schwann cell line. Expression levels for Sox10 and Cntf were estimated by measuring signal density from Western blots. A representative example is shown in G. Expression levels (mean ± SD) were quantified by using the AIDA software program. (G) Cntf and Sox10 expression in native IMS32 cells and after transient transfection of Sox10RNAiA, Sox10RNAiB, or Sox10RNAiC (see also Table 1). Sox10RNAisc is a scrambled sequence RNA interference corresponding to Sox10RNAiA that was used as a specificity control.

binding sites for specific transcription factors including Pax3, Oct6/SCIP/Tst-1, and Sox proteins (see Figs. 5 and 6A, which are published as supporting information on the PNAS web site). Comparison of the human and mouse *Cntf* promoter regions revealed that the putative Sox10 binding sites are highly conserved (Fig. 6B and C).

**Analysis of the *Cntf* Promoter by Luciferase Reporter Assays.** To characterize the role of the identified putative response elements for Pax3, Oct-6/SCIP/Tst-1, and Sox10 (see Figs. 5 and 6) in the

*Cntf* promoter, various reporter gene constructs were established (see Fig. 7A, which is published as supporting information on the PNAS web site) and transfected into the Schwann cell line IMS32, the neuroblastoma cell line Neuro2A, and the green monkey simian virus 40-transfected kidney fibroblast cell line Cos7. We have included these different cell lines in our study to investigate the regulation of *Cntf* expression in a neural cell line (Neuro2A), in a Schwann cell line (IMS32), and in a cell line not derived from the nervous system (Cos7) as a control. The Schwann cell line IMS32 was used instead of primary Schwann

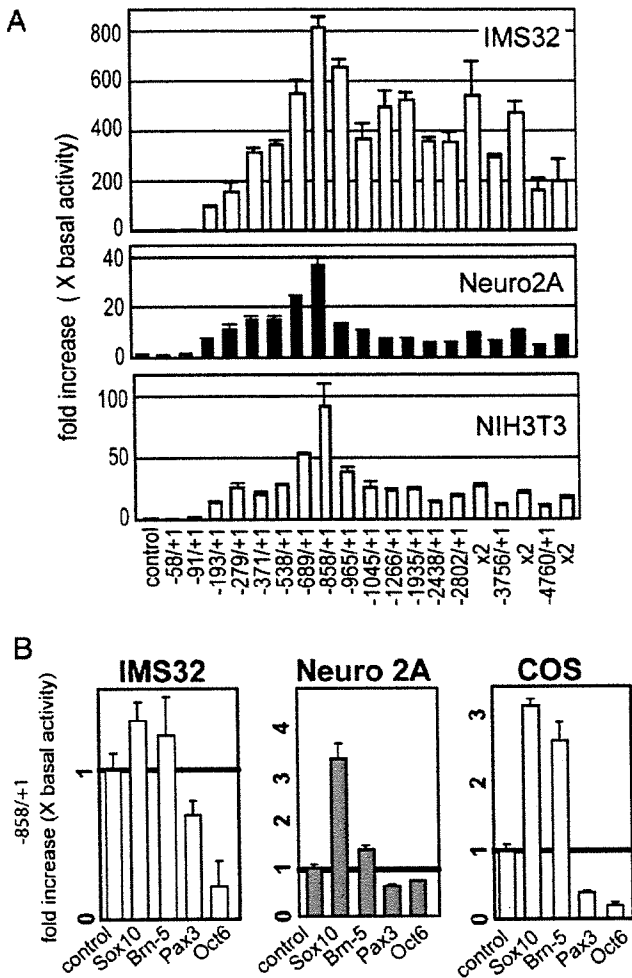


**Fig. 2.** Promoter constructs and analysis of reporter expression in various cell types. (A) Sixteen luciferase reporter constructs with different lengths of the *Cntf* promoter were generated for transient transfection in various cell lines (Fig. 7A). Transcriptional activity was determined after transfection into the Schwann cell line IMS32, Neuro2A, and NIH 3T3 cells. Relative activity was highest in IMS32 (up to 800× basal activity). The construct  $-858/+1$  revealed highest activity in all cell lines. One microgram of the reporter plasmid was used for transient transfection. As a control, empty vector was transfected. For constructs longer than 2.5 kb ( $-2,802/+1$ ,  $-3,856/+1$ , and  $-4,760/+1$ ), double amounts of plasmid were transfected to adjust for reduced number of molecules. For each construct, at least three independent transfection experiments with at least three independent plates in each experiment were performed, and luciferase activities are shown as mean  $\pm$  SD. As a control, empty vector was transfected. (B) Expression plasmids for Sox10, Brn-5, Oct-6, and Pax3 were transfected into Neuro2A, Cos7, and IMS32 cells. Data show promoter activity of the cotransfected  $-858/+1$  reporter construct relative to control (pCDNA3) transfected cells. Similar data were obtained with the  $-4,760/+1$  construct (data not shown).

cells because it was not possible to expand the primary Schwann cells at sufficient numbers for the promoter analyses. In all cell lines, the  $-858/+1$  construct showed strongest expression of the reporter (Fig. 2A) and therefore was used for subsequent analyses. Stepwise induction of gene expression was found in three regions: from base pair  $-91$  to base pair  $-193$ , from base pair  $-193$  to base pair  $-371$ , and from base pair  $-538$  to base pair  $-858$  from the ATG codon (Fig. 2A). In contrast, the region between base pair  $-371$  and base pair  $-538$  did not contribute to increased reporter gene expression. Any construct longer than

$-858/+1$  revealed no additive up-regulation. In Neuro2A and immortalized fibroblasts (NIH3T3), highly reduced reporter gene expression was observed with constructs including the base pair  $-858$  to base pair  $-965$  region. In IMS32 cells, strong reduction was recognized within a region from base pair  $-965$  to base pair  $-1,045$ . This observation could indicate that regulatory elements for transcriptional repression exist distal to base pair  $-858$ . For further studies, the  $-4,760/+1$  construct was also used because it contained the complete *Cntf* promoter including these putative repressor elements.

In the IMS32 Schwann cell line, basal levels for *Cntf* reporter gene activity were  $\approx 27$ -fold higher than in Neuro2A cells and 20-fold higher than in Cos7 cells. We then transfected the  $-856/+1$  reporter gene construct with expression plasmids for Pax3, Oct-6/SCIP/Tst-1, Sox10, and Pit-1, Oct-1, Unc-86 conserved region (POU) domain, class 6, transcription factor 1 (Brn5) (Fig. 2B). Cos7 cells do not express endogenous Pax3 (30), Oct-6/SCIP/Tst-1 (31), and Sox10 (32). Neuro2A cells do not express Pax3, Oct-6/SCIP/Tst-1, and Sox10 (2, 33). In both cell lines, transfection of Sox10 induced reporter gene expression  $\approx 3$ -fold above baseline level (Fig. 2B). In IMS32 cells, Pax3, Brn5, and Oct6/SCIP/Tst-1 are expressed endogenously (27, 34). This finding could explain why only a slight induction was observed after Sox10 or Brn5 transfection in IMS32 cells. Results were virtually identical with the  $-858/+1$  construct and the  $-4,760/+1$  promoter construct (data not shown). Brn5 led to enhanced promoter activity in Cos7 cells but not in Neuro2A or IMS32 cells. Highest induction was observed in Sox10-transfected cell lines, whereas Pax3 and Oct6 repressed *Cntf* reporter activity in all cell lines.

**Identification of Sox10 Responsive Elements in the *Cntf* Promoter.** We then performed reporter assays to further characterize Sox10-dependent activation. The Neuro2A cell line was used because it does not express Sox10 endogenously and thus could be used for cotransfection of truncated *Cntf* promoter-luciferase plasmids and Sox10-expression vectors (Fig. 3A). Sox10-dependent induction was found with constructs including regions between base pair  $-279$  and base pair  $-328$  and between base pair  $-538$  and base pair  $-858$  (Fig. 3B).

Sox10 is a high mobility group type DNA-binding protein. High mobility group proteins bind to a 7-bp consensus sequence (A/T)(A/T)CAA(A/T)G (33, 35). Such consensus elements are found at base pair positions  $-287$  and  $-293$  of the *Cntf* promoter, and two additional elements with one mismatch are localized at base pair  $-592$  to base pair  $-600$  and base pair  $-660$  to base pair  $-666$  (Fig. 5). We designated these sequences as "Sox10 high mobility group type DNA-binding motif" 1 (S1) (base pair  $-287$  to base pair  $-293$ ), S2 (base pair  $-592$  to base pair  $-600$ ), and S3 (base pair  $-660$  to base pair  $-666$ ), respectively. To evaluate the influence of Sox10 on these promoter sites, we produced mutant reporter gene constructs by replacing the consensus sequences with GCGC base pairs (see Table 1, which is published as supporting information on the PNAS web site). These mutant reporter constructs (Fig. 7B) were cotransfected with Sox10 expression plasmids into Neuro2A cells, and promoter activity was measured by luciferase assays (Fig. 3C). In comparison to the wild-type *Cntf* promoter construct, mutated S1 (S1m) showed a 56% reduction, S2m showed a modest reduction (28%), and S3 showed a weak reduction (17%). These results indicate that these putative Sox10 binding sites are important for *Cntf* expression but that their contributions are not equivalent. The S1 site appears most critical for Sox10-dependent induction. Combined mutation of all three putative Sox10 binding sites (S123m) resulted in a virtually complete loss of luciferase reporter gene induction by Sox10 (Fig. 3C).

We also performed EMSA to demonstrate direct binding of Sox10 to the S1, S2, and S3 sites. Nuclear extract from COS cells expressing Sox10 protein (Fig. 4A) showed shifted bands with a

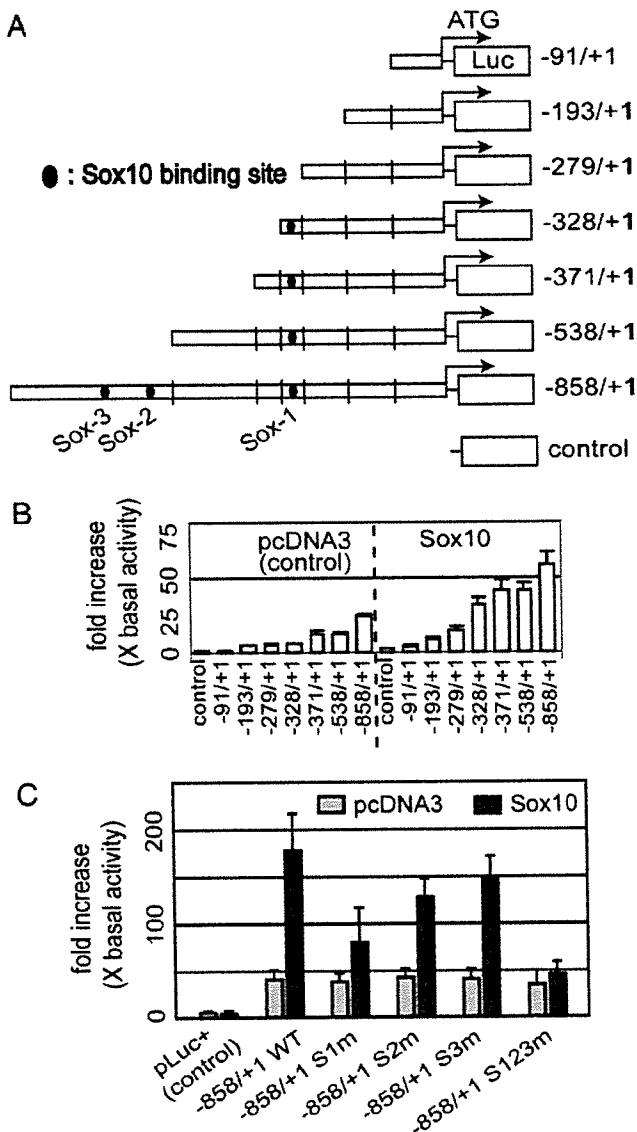


**Fig. 3.** Effect of Sox10 on *Cntf* promoter activity. (A) Cotransfection of Sox10 with *Cntf* promoter-luciferase constructs of different lengths into Neuro2A cells. The predicted Sox10 responsive regions are shown as filled circles. (B) Sox10-dependent induction was recognized between base pair -279 and base pair -328 and between base pair -538 and base pair -858. (C) Three Sox10 binding sites, S1 (base pair -287 to base pair -293), S2 (base pair -592 to base pair -600), and S3 (base pair -660 to base pair -666) were identified with mutant reporter constructs (Fig. 7B) by cotransfection with Sox10. S1m showed remarkable reduction (44%), S2m showed lower reduction (72%), and S3 showed only modest reduction (83% activity in comparison to nonmutant wild-type construct). Mutation of all three Sox10 binding sites virtually abolished Sox10-dependent promoter activity.

positive control [Sox10 consensus high mobility group type DNA-binding motif (SX)] and S1-, S2-, and S3-specific oligonucleotides (Fig. 4B). Furthermore, a supershifted band was recognized with a Sox10 antiserum for the S1 site (Fig. 4C). Weak but specific supershifted bands were also recognized for the S2 and S3 sites (results not shown). There was no oligo-protein complex recognized (Fig. 4C) with mutated oligos for the S1 site (see Table 1), indicating specificity of the supershift experiment.

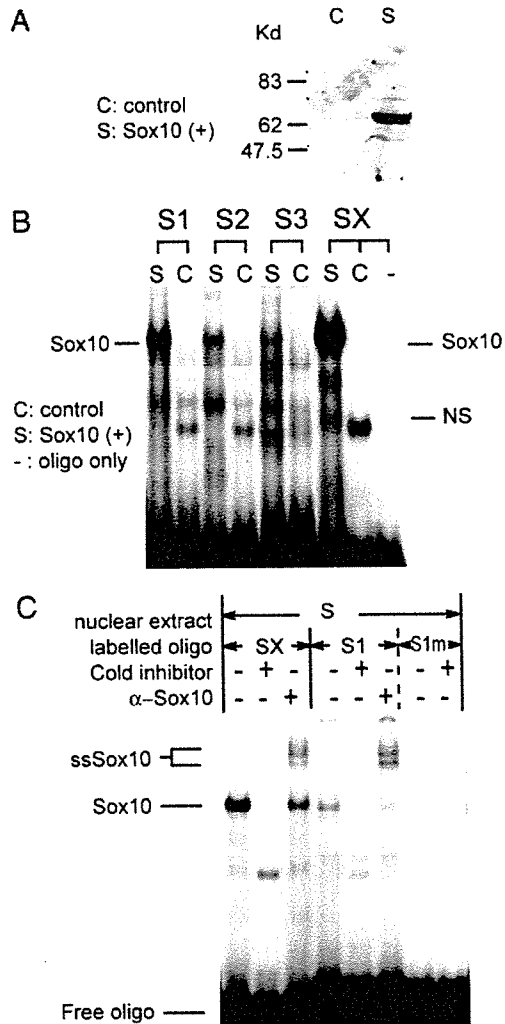


**Fig. 4.** Sox10 binding to S1, S2, and S3 sites in the *Cntf* promoter. (A) Western blot analysis of nuclear extract from COS cells transfected by Sox10 expression vector (S) and pcDNA3 control vector (C). Sox10 immunoreactivity was recognized as a single band at 64 kDa. (B) Sox10 binds to S1, S2, and S3 sites. SX is a consensus oligonucleotide for Sox10 (Table 1). S indicates the nuclear extract cotransfected with Sox10 expression vector, and C indicates the nuclear extract cotransfected with pcDNA3 empty vector. NS indicates nonspecific band. (C) A supershifted band was recognized with the Sox10 antiserum and oligonucleotide corresponding to the Sox1 site. Weak interaction was also observed for S2 and S3 (unpublished data). No oligo-protein complex recognized with mutated oligo (S1m). ssSox10, supershifted Sox10.

### Discussion

Control of myelin gene expression involves concerted actions of several transcription factors (1). Here we show that *Cntf* expression is also controlled by transcription factors previously identified in the context of Schwann cell differentiation and myelin formation. Among these, Sox10 plays a pivotal role for *Cntf* up-regulation in early postnatal Schwann cells. After birth, Sox10 expression is found at P1 and strongly increases at P3 in mice. The raise in Sox10 levels is followed by a strong increase of *Cntf* expression at P7. Moreover, the importance of Sox10 is underlined by our observation that *Cntf* protein levels are significantly reduced in sciatic nerves of *Sox10*<sup>+/-</sup> mice, even stronger than levels of P0 protein (data not shown).

Surprisingly, Pax3 appears as a repressor of *Cntf* promoter activity in our cotransfection studies. Pax3 also reduced the positive

regulatory effect of Sox10. Pax3 is indispensable for the differentiation of neural crest derivatives (36). Its expression in peripheral nerves of embryonic mice is high, and expression goes down around birth before Cntf expression is up-regulated. It appears tempting to speculate that Pax3 represses expression of Cntf during embryonic development and that the down-regulation of Pax3 around birth contributes to the massive up-regulation of Cntf production starting in the first postnatal week.

Interestingly, patients with deletion or mutations in the *Sox10* gene reveal defects in the peripheral nervous system known as Hirschsprung disease (37, 38). In such patients, defects of the enteric ganglia and subsequently a lack of coordinated innervation of bowel and gut are prevailing, but peripheral neuropathies are also part of the disease phenotype (39). It is not clear whether the neuropathy can simply be explained as a defect in proper myelination in such patients (40). It is likely that Sox10 controls additional target genes that influence maintenance and function of the peripheral nervous system. Thus, reduced Cntf levels could contribute to this phenotype. Levels of Cntf protein in human peripheral nerves are much lower than in mice (M.S., unpublished observations), and human CNTF is less active than the mouse Cntf protein, even in human target cells (41). Thus, reduced gene expression might be more critical in humans in comparison to mice. In postnatal *Cntf*<sup>-/-</sup> mice, loss of motoneurons occurs (17), and degenerative alterations in Schwann cell morphology such as disintegration of paranodal networks are detectable at nodes of Ranvier (42). Furthermore, reduced Cntf levels exaggerate the disease phenotype when combined with the *superoxide dismutase 1* (*SOD1*) (19) gene mutation resulting in more severe motoneuron disease. Thus, reduced Cntf expression might also be relevant for the pathophysiology of neuropathies caused by mutations in *Sox10* or other conditions reducing Sox10 levels.

In summary, our data indicate that Sox10 up-regulates *Cntf* gene expression in Schwann cells and other cell types and that Cntf protein levels are reduced in *Sox10* mutant mice. Dysregulation of Cntf expression could contribute to the phenotype of specific neuropathies, in particular those caused by mutations in *Sox10*.

## Materials and Methods

**Cloning and Sequencing of Murine *Cntf* Promoter.** A genomic clone containing a 6.5-kb insert with the complete *Cntf* gene was obtained by screening bacterial artificial chromosome filters (Incyte Genomics, Palo Alto, CA). Digestion of a positive bacterial artificial chromosome with EcoRV, subcloning into pBSII KS+/-, and DNA sequencing revealed that this clone also contained the 4.7-kb 5' promoter region of *Cntf* including the 3' region of the *Zfp* gene, which is located upstream of *Cntf*.

**Computer Analysis of Putative Binding Sites for Transcription Factors in the *Cntf* Promoter.** Programs provided by the Genetics Computer Group (Madison, WI) and MATINSPECTOR PROFESSIONAL (Genomatix, Munich) (43) were used for sequence analysis of the *Cntf* promoter.

**RNA Extraction, 5' and 3' RACE (Oligo Cap Methods).** Total RNA was isolated from adult mouse sciatic nerve by TRIzol (Invitrogen) according to the manufacturer's protocol. The 5' and 3' RACE

were performed as described in *Supporting Methods*, which is published as supporting information on the PNAS web site.

**Plasmid Constructs, Cell Culture, Transfection, and Luciferase Assays.** DNA corresponding to various regions of the *Cntf* promoter was cloned by PCR with appropriate sense and antisense primers (Cz10rev2) (Table 2, which is published as supporting information on the PNAS web site). Cloning of expression and reporter constructs is described in *Supporting Methods*.

NIH 3T3, Cos7, Neuro2A, and IMS32 Schwann cell lines (27) and primary Schwann cells were maintained in Dulbecco-Vogt-modified Eagle's medium with 10% FCS, 50 units/ml penicillin, and 100 µg/ml streptomycin. Transfection was performed as described in *Supporting Methods* and Table 1.

**Nuclear Protein Extraction and Western Blotting.** Cos7 and Neuro2A cells were transfected with 37.5 µg of expression vectors for Sox10 in 100-mm dishes. In parallel, pcDNA3 vector was transfected as a control. After 24 h, cells were harvested, and nuclear extracts were collected (44). Protein concentration was measured by using a Bradford assay. Nuclear protein extracts (25 µg) were subjected to Western blotting. Anti-Sox10 antibody (45) was used at a 1:3,000 dilution. The Cntf antiserum K10 was used at a 1:5,000 dilution. Recombinant rat Cntf was used as a standard for analysis of Cntf expression levels.

**EMSA.** Double-stranded 30- or 34-bp oligonucleotides (1 µg) were radiolabeled by extension of overhanging GATC 4-bp ends with Klenow fragment of DNA polymerase in the presence of [ $\alpha$ -<sup>32</sup>P]dCTP. Labeled oligonucleotide and 4 µg of nuclear protein were incubated in 20 µl of reaction mixture. Reaction mixture for Sox10 contained 10 mM Hepes (pH 8.0), 50 mM NaCl, 5 mM MgCl<sub>2</sub>, 0.1 mM EDTA, 2 mM DTT, 5% glycerol, 10% BSA, and 2 µg of poly[d(I)d(C)] (Sigma). For competition experiments, unlabeled double-stranded oligonucleotides were preincubated in 250-fold excess with the protein for 20 min before labeled oligonucleotides were added. Supershifts were performed by using an antibody to Sox10 as described (45). All samples were electrophoresed on 5% native polyacrylamide gels for 1.5 h at 140 V. Gels were dried after electrophoresis and exposed to X-OMAT film (Kodak) to detect radioactivity.

**Western Blot Analysis.** Sciatic nerves were dissected from P1, P3, P7, and P42 wild-type and *Sox10*<sup>+/-</sup> mice (8). Cell lysates from Sox10 RNA interference-transfected IMS32 cells were harvested 24 h after transfection. Protein extracts were prepared and processed for Cntf and Sox10 (46) Western blot analysis. Blots were then stripped and reacted with antibodies against actin (MAB1501R; Chemicon). Signal intensities were measured and normalized against the actin signal (AIDA software package; Raytest, Straubenhardt, Germany). Statistical analysis was performed by using the unpaired two-tailed *t* test (PRISM; GraphPad, San Diego).

We thank Michaela Pfister for technical assistance. This work was supported by the Deutsche Forschungsgemeinschaft (SFB581), grants from the Japan Foundation for Aging and Health (to Y.I.), and the Kanae Foundation for Life & Socio-Medical Science.

1. Wegner, M. (2000) *Glia* 29, 118–123.
2. Kioussi, C., Gross, M. K. & Gruss, P. (1995) *Neuron* 15, 553–562.
3. Monuki, E. S., Weinmaster, G., Kuhn, R. & Lemke, G. (1989) *Neuron* 3, 783–793.
4. Jaegle, M., Mandemakers, W., Broos, L., Zwart, R., Karis, A., Visser, P., Grosveld, F. & Meijer, D. (1996) *Science* 273, 507–510.
5. Bermingham, J. R., Jr., Scherer, S. S., O'Connell, S., Arroyo, E., Kalla, K. A., Powell, F. L. & Rosenfeld, M. G. (1996) *Genes Dev.* 10, 1751–1762.
6. Arroyo, E. J., Bermingham, J. R., Jr., Rosenfeld, M. G. & Scherer, S. S. (1998) *J. Neurosci.* 18, 7891–7902.

7. Kuhlbrodt, K., Schmidt, C., Sock, E., Pingault, V., Bondurand, N., Goossens, M. & Wegner, M. (1998) *J. Biol. Chem.* 273, 23033–23038.
8. Britsch, S., Goerich, D. E., Riethmacher, D., Peirano, R. L., Rossner, M., Nave, K. A., Birchmeier, C. & Wegner, M. (2001) *Genes Dev.* 15, 66–78.
9. Stöckli, K. A., Lottspeich, F., Sendtner, M., Masiakowski, P., Carroll, P., Götz, R., Lindholm, D. & Thoenen, H. (1989) *Nature* 342, 920–923.
10. Stöckli, K. A., Lillien, L. E., Näher-Noe, M., Breitfeld, G., Hughes, R. A., Thoenen, H. & Sendtner, M. (1991) *J. Cell Biol.* 115, 447–459.
11. Stahl, N. & Yancopoulos, G. D. (1994) *J. Neurobiol.* 25, 1454–1466.
12. Ip, N. Y. & Yancopoulos, G. D. (1996) *Annu. Rev. Neurosci.* 19, 491–515.

13. Bonni, A., Sun, Y., Nadal-Vicens, M., Bhatt, A., Frank, D. A., Rozovsky, I., Stahl, N., Yancopoulos, G. D. & Greenberg, M. E. (1997) *Science* 278, 477–483.
14. Sendtner, M., Kreutzberg, G. W. & Thoenen, H. (1990) *Nature* 345, 440–441.
15. Sendtner, M., Stöckli, K. A. & Thoenen, H. (1992) *J. Cell Biol.* 118, 139–148.
16. Sendtner, M., Götz, R., Holtmann, B. & Thoenen, H. (1997) *J. Neurosci.* 17, 6999–7006.
17. Masu, Y., Wolf, E., Holtmann, B., Sendtner, M., Brem, G. & Thoenen, H. (1993) *Nature* 365, 27–32.
18. DeChiara, T. M., Vejsada, R., Poueymirou, W. T., Acheson, A., Suri, C., Conover, J. C., Friedman, B., McClain, J., Pan, L., Stahl, N., *et al.* (1995) *Cell* 83, 313–322.
19. Giess, R., Holtmann, B., Braga, M., Grimm, T., Müller-Myhsok, B., Toyka, K. V. & Sendtner, M. (2002) *Am. J. Hum. Genet.* 70, 1277–1286.
20. Giess, R., Maurer, M., Linker, R., Gold, R., Warmuth-Metz, M., Toyka, K. V., Sendtner, M. & Rieckmann, P. (2002) *Arch. Neurol. (Chicago)* 59, 407–409.
21. Linker, R. A., Maurer, M., Gaupp, S., Martini, R., Holtmann, B., Giess, R., Rieckmann, P., Lassmann, H., Toyka, K. V., Sendtner, M., *et al.* (2002) *Nat. Med.* 8, 620–624.
22. Sendtner, M., Schmalbruch, H., Stöckli, K. A., Carroll, P., Kreutzberg, G. W. & Thoenen, H. (1992) *Nature* 358, 502–504.
23. Mitsumoto, H., Ikeda, K., Holmlund, T., Greene, T., Cedarbaum, J. M., Wong, V. & Lindsay, R. M. (1994) *Ann. Neurol.* 36, 142–148.
24. Dobra, G. M., Unnerstall, J. R. & Rao, M. S. (1992) *Dev. Brain Res.* 66, 209–219.
25. Herbarth, B., Pingault, V., Bondurand, N., Kuhlbrodt, K., Hermans-Borgmeyer, I., Puliti, A., Lemort, N., Goossens, M. & Wegner, M. (1998) *Proc. Natl. Acad. Sci. USA* 95, 5161–5165.
26. Southard-Smith, E. M., Kos, L. & Pavan, W. J. (1998) *Nat. Genet.* 18, 60–64.
27. Watabe, K., Fukuda, T., Tanaka, J., Honda, H., Toyohara, K. & Sakai, O. (1995) *J. Neurosci. Res.* 41, 279–290.
28. Saotome, Y., Winter, C. G. & Hirsh, D. (1995) *Gene* 152, 233–238.
29. Carroll, P., Sendtner, M., Meyer, M. & Thoenen, H. (1993) *Glia* 9, 176–187.
30. Pritchard, C., Grosveld, G. & Hollenbach, A. D. (2003) *Gene* 305, 61–69.
31. Faus, I., Hsu, H. J. & Fuchs, E. (1994) *Mol. Cell. Biol.* 14, 3263–3275.
32. Schlierf, B., Ludwig, A., Klenovsek, K. & Wegner, M. (2002) *Nucleic Acids Res.* 30, 5509–5516.
33. Peirano, R. I., Goerich, D. E., Riethmacher, D. & Wegner, M. (2000) *Mol. Cell. Biol.* 20, 3198–3209.
34. Watabe, K., Sakamoto, T., Kawazoe, Y., Michikawa, M., Miyamoto, K., Yamamura, T., Saya, H. & Araki, N. (2003) *Neuropathology* 23, 68–78.
35. Wegner, M. (1999) *Nucleic Acids Res.* 27, 1409–1420.
36. Goulding, M. D., Chalepakis, G., Deutsch, U., Erselius, J. R. & Gruss, P. (1991) *EMBO J.* 10, 1135–1147.
37. Tassabehji, M., Read, A. P., Newton, V. E., Harris, R., Balling, R., Gruss, P. & Strachan, T. (1992) *Nature* 355, 635–636.
38. Hoth, C. F., Milunsky, A., Lipsky, N., Sheffer, R., Clarren, S. K. & Baldwin, C. T. (1993) *Am. J. Hum. Genet.* 52, 455–462.
39. Cheng, W., Au, D. K., Knowles, C. H., Anand, P. & Tam, P. K. (2001) *J. Pediatr. Surg.* 36, 296–300.
40. Inoue, K., Shilo, K., Boerkoel, C. F., Crowe, C., Sawady, J., Lupski, J. R. & Agamanolis, D. P. (2002) *Ann. Neurol.* 52, 836–842.
41. Wong, V., Pearsall, D., Arriaga, R., Ip, N. Y., Stahl, N. & Lindsay, R. M. (1995) *J. Biol. Chem.* 270, 313–318.
42. Gatzinsky, K. P., Holtmann, B., Daraic, B., Berthold, C. H. & Sendtner, M. (2003) *Glia* 42, 340–349.
43. Ouandi, K., Frech, K., Karas, H., Wingender, E. & Werner, T. (1995) *Nucleic Acids Res.* 23, 4878–4884.
44. Sock, E., Leger, H., Kuhlbrodt, K., Schreiber, J., Enderich, J., Richter-Landsberg, C. & Wegner, M. (1997) *J. Neurochem.* 68, 1911–1919.
45. Kuhlbrodt, K., Herbarth, B., Sock, E., Enderich, J., Hermans-Borgmeyer, I. & Wegner, M. (1998) *J. Biol. Chem.* 273, 16050–16057.
46. Stolt, C. C., Lommes, P., Sock, E., Chaboissier, M. C., Schedl, A. & Wegner, M. (2003) *Genes Dev.* 17, 1677–1689.



## High glucose-induced activation of the polyol pathway and changes of gene expression profiles in immortalized adult mouse Schwann cells IMS32

Kazunori Sango,\* Takeshi Suzuki,† Hiroko Yanagisawa,\* Shizuka Takaku,\* Hiroko Hirooka,† Miyuki Tamura† and Kazuhiko Watabe‡

\*Department of Developmental Morphology, Tokyo Metropolitan Institute for Neuroscience, Fuchu, Tokyo, Japan

†Pharmaceutical Research Laboratories, Sanwa Kagaku Kenkyusho Co. Ltd, Inabe, Japan

‡Department of Molecular Neuropathology, Tokyo Metropolitan Institute for Neuroscience, Fuchu, Tokyo, Japan

### Abstract

We investigated the polyol pathway activity and the gene expression profiles in immortalized adult mouse Schwann cells (IMS32) under normal (5.6 mM) and high (30 and 56 mM) glucose conditions for 7–14 days in culture. Messenger RNA and the protein expression of aldose reductase (AR) and the intracellular sorbitol and fructose contents were up-regulated in IMS32 under high glucose conditions compared with normal glucose conditions. By employing DNA microarray and subsequent RT-PCR/northern blot analyses, we observed significant up-regulation of the mRNA expressions for serum amyloid A3 (SAA3), angiopoietin-like 4 (ANGPTL4) and ecotropic viral integration site 3 (Evi3), and the down-regulation of aldehyde reductase (AKR1A4) mRNA expression in the cells

under high glucose (30 mM) conditions. The application of an AR inhibitor, SNK-860, to the high glucose medium ameliorated the increased sorbitol and fructose contents and the reduced AKR1A4 mRNA expression, while it had no effect on mRNA expressions for SAA3, ANGPTL4 or Evi3. Considering that the exposure to the high glucose ( $\geq 30$  mM) conditions mimicking hyperglycaemia *in vivo* accelerated the polyol pathway in IMS32, but not in other previously reported Schwann cells, the culture system of IMS32 under those conditions may provide novel findings about the polyol pathway-related abnormalities in diabetic neuropathy.

**Keywords:** aldehyde reductase, diabetic neuropathy, DNA microarray, immortalized Schwann cells, polyol pathway.

*J. Neurochem.* (2006) 10.1111/j.1471-4159.2006.03885.x

Peripheral neuropathy is one of the most common complications of diabetes mellitus, as are retinopathy and nephropathy. Both metabolic alterations in the cellular components (mainly neurons and Schwann cells) and microvascular abnormalities are thought to play major roles in the development of diabetic neuropathy (Mizisin and Powell 2003), although the detailed pathogenesis remains unclear. Schwann cells are responsible for the action potential velocity through the insulation of axons, the maintenance of axonal caliber, effective nerve regeneration after axonal injury and other neural functions in the peripheral nervous system (Eckersley 2002). Therefore, Schwann cell abnormalities as a result of hyperglycaemia can be a cause of nerve dysfunction, such as reduced nerve conduction velocity, axonal atrophy and impaired axonal regeneration (Dyck and Giannini 1996; Song *et al.* 2003; Yasuda *et al.* 2003). The role of Schwann cells in diabetic neuropathy is often

discussed in relation to polyol pathway hyperactivity (Eckersley 2002; Mizisin and Powell 2003). Aldose reductase (AR; EC 1.1.1.21) is the first enzyme in the polyol pathway and converts glucose to sorbitol using NADPH as a

Received September 27, 2005; revised manuscript received January 8, 2006; accepted March 5, 2006.

Address correspondence and reprint requests to Kazunori Sango, Department of Developmental Morphology, Tokyo Metropolitan Institute for Neuroscience, 2–6 Musashidai, Fuchu, Tokyo 183–8526, Japan. E-mail: kzsango@tmin.ac.jp

**Abbreviations used:** ADH, alcohol dehydrogenase; AKR, aldo-keto reductase; ALDH, aldehyde dehydrogenase; ANGPTL4, angiopoietin-like 4; AR, aldose reductase; DRG, dorsal root ganglia; Evi3, ecotropic viral integration site 3; LPL, lipoprotein lipase; NO, nitric oxide; PPAR, peroxisome proliferator-activated receptor; p75<sup>NTR</sup>, p75 low-affinity nerve growth factor receptor; SAA3, serum amyloid A3; SDH, sorbitol dehydrogenase; STZ, streptozotocin.

cofactor. Because AR is localized to Schwann cells in the peripheral nerves (Kern and Engerman 1982), it has been proposed that the activation of AR in Schwann cells under hyperglycaemic conditions affects nerve functions through various mechanisms: (i) sorbitol accumulation leads to osmotic stress and the depletion of myo-inositol and taurine (Tomlinson 1999; Pop-Busui *et al.* 2001); (ii) the increase in AR activity competes with nitric oxide (NO) synthase or glutathione reductase for NADPH. The inhibition of NO synthase and the subsequent decrease in NO in the nervous tissue causes diminished nerve flow, whereas the depletion of reduced glutathione by glutathione reductase inhibition results in the excessive production of free radicals (Low *et al.* 1999); (iii) sorbitol is converted to fructose by sorbitol dehydrogenase (SDH, EC 1.1.1.14), the second enzyme in the polyol pathway. Fructose and its metabolites, such as fructose-6-phosphate and triose-phosphate, can be triggers of non-enzymatic glycation of cellular proteins and lipids (Takagi *et al.* 1995).

Culture systems of Schwann cells appear to be useful for investigating the role of polyol pathway hyperactivity in the pathogenesis of diabetic neuropathy. Thus far, an established Schwann cell line, JS1 (Mizisin *et al.* 1996), and primary cultured adult rat Schwann cells (Suzuki *et al.* 1999; Maekawa *et al.* 2001) have been introduced to study polyol metabolism, but these cells did not display intracellular sorbitol accumulation or enhanced AR expression/enzyme activity under high glucose (25–30 mM) conditions unless hyperosmotic stress (greater than 100 mM) was applied. The reasons for this remain unknown. We have established a spontaneously immortalized Schwann cell line, IMS32, from long-term cultures of adult mouse dorsal root ganglia (DRG) and peripheral nerves (Watabe *et al.* 1995). Because IMS32 possesses some biological properties of mature Schwann cells and high proliferation activity (Watabe *et al.* 1995; Sango *et al.* 2004), this cell line is suitable for functional and biochemical studies of the peripheral nervous system. Kato and colleagues reported that the proliferation activity of IMS32 was decreased by exposure to high glucose (20–40 mM) conditions (Kato *et al.* 2003; Nakamura *et al.* 2003), but the polyol metabolism in the cells has not yet been characterized. If the polyol pathway is activated in IMS32 in response to the high glucose concentrations mimicking hyperglycaemia *in vivo*, this cell line would be a valuable tool for the study of diabetic neuropathy. In the present study, we investigated the mRNA expression of AR and SDH, the protein expression of AR and the intracellular contents of sorbitol and fructose in IMS32 under high glucose (30 and 56 mM) and hyperosmotic (50 mM of sodium chloride) conditions. We also employed DNA microarray and subsequent RT-PCR/northern blot analyses to see the high glucose (30 mM)-induced alterations in the gene expression profiles, especially in association with the polyol pathway activity.

## Materials and methods

### Preparation of the plasmid-containing mouse cDNAs for AR and SDH

The plasmids containing mouse AR and SDH cDNA fragments were created by PCR cloning, as described previously (Sango *et al.* 2004). Briefly, total RNA was isolated from IMS32 using Sepazol reagent (Nacalai Tesque, Kyoto, Japan), and was reverse transcribed with M-MLV reverse transcriptase (Invitrogen, Groningen, the Netherlands) and pd(N)<sub>6</sub> random primer (Amersham Pharmacia Biotech, Piscataway, NJ, USA). The synthesized cDNA was used as a template for the PCR reaction. The PCR primers were designed to amplify the 896 bp of mouse AR [aldo-keto reductase 1B3 (AKR1B3)] gene (sense primer 5'-ATGGCCAGCCATCTGGAACTC-3' and antisense primer 5'-CACACCTCCAGTTCCTGTT-3') (GenBank accession no. NM\_009658) and the 1074 bp of mouse SDH gene (sense primer 5'-ATGGCAGCTCCAGCTAAGGC-3' and antisense primer 5'-CTAGGGGTTTTGGTCATTGGG-3') (GenBank accession no. NM\_146126). The PCR products were subcloned into pGEM-T Easy Vector (Promega, Madison, WI, USA) according to the manufacturer's instructions, and the resulting plasmid DNA was sequenced (Promega/Bex Co. Ltd, Tokyo, Japan).

### Cell culture

Immortalized adult mouse Schwann cells (IMS32) were seeded on 75-cm<sup>2</sup> flasks (Nalge Nunc International, Naperville, IL, USA) at a density of  $5 \times 10^4$ /cm<sup>2</sup> and cultured in Dulbecco's modified Eagle's medium (DMEM; Sigma, St Louis, MO, USA) supplemented with 10% fetal calf serum (FCS; Invitrogen). The medium contained 5.6 mM glucose. When the cells reached approximately 80–85% confluency, they were maintained in DMEM supplemented with 1% FCS and containing 5.6 mM glucose (Glc-5.6), 30 mM glucose (Glc-30), 56 mM glucose (Glc-56) or 5.6 mM glucose and 50 mM sodium chloride (NaCl-50). The media containing a low concentration (1%) of serum slowed the proliferation of IMS32, and made it possible to keep the cultures in the same culture flasks for up to 14 days without detachment and the re-seeding of cells. Seven days after incubation under each experimental condition, the cells were rinsed with phosphate-buffered saline (PBS, Sigma) and detached from the flasks by cell scrapers (Sumitomo Bakelite Co. Ltd, Tokyo, Japan). These cells were suspended in 2 mL of sterile water and collected in sterile tubes for use in northern blotting or western blotting.

### Northern blotting

The cDNA fragments of AR and SDH (10 ng/mL) were prepared from the plasmids, and labelled with alkaline phosphatase [AlkPhos Direct (Amersham Pharmacia Biotech)] according to the manufacturer's instructions. Total RNA was isolated from the cells using Sepazol reagent, and the concentration of RNA was determined with a spectrophotometer (Gene Quant Pro; Amersham Pharmacia Biotech). Twenty-five micrograms of total RNA was electrophoresed in 1% agarose-formaldehyde gel and transferred to Hybond N+ membrane (Amersham Pharmacia Biotech). We prepared two membranes with the same RNA samples; one was stained with methylene blue (Waldeck-GmbH and Co KG, Münster, Germany) and the other was hybridized overnight at 50°C with the labelled probes. The CDP-Star<sup>TM</sup> chemiluminescent detection reagent and

Hyperfilm ECL (Amersham Pharmacia Biotech) were used for visualization of the positive signals (Sango *et al.* 2004). The band intensity was quantified with Edas 290 1D Image Analysis software (Eastman Kodak, New York, NY, USA; Sango *et al.* 2002), and the abundance of mRNA was expressed as a 'relative expression' (the intensity in each experimental group relative to that in Glc-5.6). 28S ribosomal RNA stained with methylene blue on the duplicate membranes was used for standardization.

#### Western blotting

Cells were homogenized with a cell sonicator (Tomy Seiko Co. Ltd, Tokyo, Japan), and the concentration of protein was determined by using a DC Protein Assay (Bio-Rad Laboratories, Hercules, CA, USA) according to the manufacturer's instructions. Twenty micrograms of protein were electrophoresed on 14–16% gradient sodium dodecyl sulfate – polyacrylamide gel electrophoresis (Daiichi Pure Chemical Co. Ltd, Tokyo, Japan) under non-reducing conditions and transferred to nitrocellulose paper (Bio-Rad Laboratories). The blotted paper was then blocked with 5% skimmed milk and incubated for 1 h at room temperature (25°C) with goat polyclonal anti-AR antibody [ALR2 (P-20), 1 : 2000; Santa Cruz Biotechnology, Santa Cruz, CA, USA] or mouse monoclonal anti- $\beta$ -actin antibody (1 : 1000; Sigma), followed by incubations with biotinylated anti-goat IgG or anti-mouse IgG (1 : 1000; Vector Laboratories, Burlingame, CA, USA), and streptavidin-alkaline phosphatase (1 : 1000; Promega). Reactions were visualized by colour development using Western blue<sup>®</sup> stabilized substrate for alkaline phosphatase (Promega).

#### Immunocytochemistry

IMS32 were seeded on wells of 8-well chamber slides (Nalge Nunc) or Aclar fluorocarbon coverslips (Nissin EM Co. Ltd, Tokyo, Japan; 9 mm in diameter) at a density of  $1-2 \times 10^4/\text{cm}^2$ , and kept in Glc-5.6, Glc-30, Glc-56 or NaCl-50 for 7 days. Then, the cells were fixed with 4% paraformaldehyde for 15 min at 4°C with the following antibodies (diluted with 20 mM PBS containing 0.5% skimmed milk): (i) goat anti-AR polyclonal antibody (1 : 3000); (ii) rabbit anti-S100 polyclonal antibody (1 : 3000; Dako, Carpinteria, CA, USA); (iii) rabbit anti-p75 low-affinity nerve growth factor receptor (p75<sup>NTR</sup>) polyclonal antibody (1 : 1000; Promega).

After rinsing with PBS, the cells were incubated for 1 h at 37°C with peroxidase-conjugated anti-goat IgG (for AR) or anti-rabbit IgG (for S100 and p75<sup>NTR</sup>) antibody (1 : 100, Vector Laboratories). The immunoreaction was visualized under a light microscope using 0.01% diaminobenzidine tetrahydro-chloride (DAB; Wako Co., Tokyo, Japan) and 0.01% hydrogen peroxide in 50 mM Tris buffer (pH 7.4) at room temperature for 15 min (Sango *et al.* 2004).

#### Measurement of the intracellular contents of sorbitol and fructose

IMS32 were seeded on wells of 6-well plates (Corning Inc., Corning, NY, USA) at a density of  $5 \times 10^4/\text{cm}^2$ , and kept in Glc-5.6 or Glc-30 for 14 days. A subset of Glc-30 was treated with 1  $\mu\text{M}$  of an AR inhibitor, SNK-860 (Sanwa Kagaku Kenkyusho Co. Ltd, Inabe, Japan) for 7 days (from 7 to 14 days in culture). This culture condition was termed Glc-30/SNK. Cells under each experimental condition were rinsed in ice-cold PBS and homogenized in 2 mL of cold water with a cell sonicator. Protein concentrations were

determined by using a DC Protein Assay (Bio-Rad Laboratories) according to the manufacturers' instructions. The polyol level in each lyophilized sample was determined by liquid chromatography with tandem mass spectrometry, according to the method of Guerrant and Moss (1984). The value of polyol was expressed as nmol/mg protein.

#### DNA microarray analysis

IMS32 cells were kept in Glc-5.6 or Glc-30 for 14 days in 175-cm<sup>2</sup> flasks (Nalge Nunc), and the total RNA was isolated from the cells using an RNeasy mini kit (Qiagen, Tokyo, Japan). The DNA microarray analysis was performed with these samples (Custom Technology Service by Kurabo Industries Ltd, Osaka, Japan). Briefly, total RNA was reverse transcribed to cDNA with T7 oligo d(T) primer (Amersham Pharmacia Biotech). The cDNA synthesis product was used in an *in vitro* transcription reaction containing T7 RNA polymerase and biotinylated uridine triphosphate. Then, the labelled cRNA products were fragmented, loaded onto CodeLink<sup>™</sup> Uniset Mouse 20K Bioarray (Amersham Pharmacia Biotech) and hybridized according to the manufacturer's protocol. Streptavidin-Cy5 (Amersham Pharmacia Biotech) was used as the fluorescent conjugate to detect hybridized target sequences. Raw intensity data from the CodeLink Bioarray were analyzed in Microsoft Excel (Microsoft, Redmond, WA, USA) and gene expression levels were expressed as relative intensities (intensity data in Glc-30 compared with those in Glc-5.6). Only the fold changes of relative intensities >2.0 and <0.5 were considered to be significant up-regulations and down-regulations, respectively.

#### Confirmation of high glucose-responsive gene expression by RT-PCR and northern blot analyses

Total RNA was isolated from the cells kept in Glc-5.6, Glc-30 or Glc-30/SNK for 14 days in 75-cm<sup>2</sup> flasks by using Sepazol reagent. Semi-quantitative RT-PCR analysis was carried out as described previously (Sango *et al.* 2002). Briefly, first-strand cDNA was synthesized from 4  $\mu\text{g}$  of total RNA and PCR amplification was performed in a reaction volume of 25  $\mu\text{L}$  containing 2  $\mu\text{L}$  of diluted cDNA, 0.625 U of AmpliTaqGold<sup>™</sup> DNA polymerase (Applied Biosystems, Foster City, CA, USA), each dNTP at 0.2 mM, 50 mM KCl, 10 mM Tris-HCl (pH 8.3), 1.5 mM MgCl<sub>2</sub> and sense and antisense primers each at 0.5  $\mu\text{M}$ . Oligonucleotide sense and antisense primers for the PCR were as follows: serum amyloid A3 (SAA3; GenBank accession no. NM\_011315), 5'-ATGAA-GCCTCCATTGCCA-3' and 5'-TATCTTTTAGGCAGGCAGGC-CAGCA-3' (a 365-bp product); angiotensin-like 4 (ANGPTL4; GenBank accession no. NM\_020581), 5'-AGGGGCCCAAGGG-AAAAGAT-3' and 5'-TAGCCTCCATGGGCTGGAT-3' (a 978-bp product); ecotropic viral integration site 3 (Evi3; GenBank accession no. NM\_145492), 5'-TGGGGAGGCAGTAGACTG-3' and 5'-CTCCATCCTGGAGCCAGA-3' (a 640-bp product);  $\beta$ -actin (the internal standard; GenBank accession no. NM\_007393), 5'-AGA-AGCTGTGCTATGTTGCC-3' and 5'-ATCCACACAGACTACTT-GCC-3' (a 382-bp product).

All PCR reactions were carried out under conditions in which the amplification was linear by using the appropriate number of cycles. The PCR products were resolved by electrophoresis in a 2% agarose gel at 100 V for 30 min. The intensity of the PCR fragments visualized by ethidium bromide staining were quantified with

Edas 290, and the abundance of the respective mRNAs was expressed as the intensity of each cDNA fragment/intensity of the  $\beta$ -actin cDNA fragment.

For northern blot analysis, the plasmid-containing mouse aldehyde reductase (AKR1A4; GenBank accession no. NM\_021473) cDNA fragment was created by PCR cloning with the following primers: 5'-TCCAGTGTCTCCTGCACA-3' and 5'-TCAGTATGGTTCATTAAGGG-3' (a 969-bp product).

#### mRNA expression of SAA3, ANGPTL4, Evi3 and AKR1A4 in the peripheral nerves of adult mice

Three-month-old female ICR mice were anaesthetized by ether and killed, in accordance with the Guideline for the Care and Use of Animals (Tokyo Metropolitan Institute for Neuroscience). Thirty dorsal root ganglia (from the thoracic to sacral levels) with associated spinal nerve bundles were dissected from each mouse, and total RNA was isolated from the dissected tissue as previously described (Sango *et al.* 2002). The cDNA synthesis and subsequent RT-PCR analysis was carried out as described above, using the PCR primers for SAA3, ANGPTL4, Evi3 and AKR1A4.

#### Statistical analysis

For statistical comparison, post-hoc tests were performed using Bonferroni/Dunn post-hoc analyses. *p*-values of <0.05 were considered significant.

## Results

#### IMS32 exhibited Schwann cell phenotypes under normal and high glucose conditions

IMS32 cells showed distinct Schwann cell phenotypes, such as the spindle-shaped morphology (Figs 1a–c) and the

expression of Schwann cell markers such as S100 (Figs 1d–f) and p75<sup>NTR</sup> (not shown) under normal (Glc-5.6; Figs 1a and d) and high glucose conditions (Glc-30 and Glc-56; Figs 1b and e, and Figs 1c and f, respectively). We observed no significant difference in the morphological appearances of living cells or immunoreactivity to S100/p75<sup>NTR</sup> between Glc-5.6 and Glc-30 or Glc-56. The application of SNK-860 to the high glucose conditions failed to alter these phenotypes of IMS32 (not shown).

#### Up-regulated AR and SDH mRNA expressions in IMS32 under the high glucose and hyperosmotic conditions

By northern blot analysis with alkaline-phosphatase-labelled cDNA probes, mRNA for AR and SDH were detected as single bands corresponding to the molecular weight of around 1.4 and 2.4 kb molecular size, respectively (Fig. 2a, upper). These results were consistent with those in the previous studies (Gui *et al.* 1995; Lee *et al.* 1995). The blot showed more intense signals for AR mRNA in Glc-30, Glc-56 and NaCl-50 than those in Glc-5.6, and for SDH mRNA in Glc-56 and NaCl-50 than those in Glc-5.6. Methylene blue-stained images of the duplicate membrane (Fig. 2a, lower) showed that a relatively equal amount of RNA was loaded. The average values of the relative expression of AR mRNA were 1 in Glc-5.6, 1.88 in Glc-30, 2.41 in Glc-56 and 2.78 in NaCl-50, respectively (Fig. 2b); AR mRNA expression was up-regulated under the high glucose (Glc-30 and Glc-56) and hyperosmotic (NaCl-50) conditions, although the difference in the values between Glc-30 and Glc-5.6 was not statistically significant. The average values of relative expression of SDH mRNA were 1 in Glc-5.6, 1.19 in Glc-30,

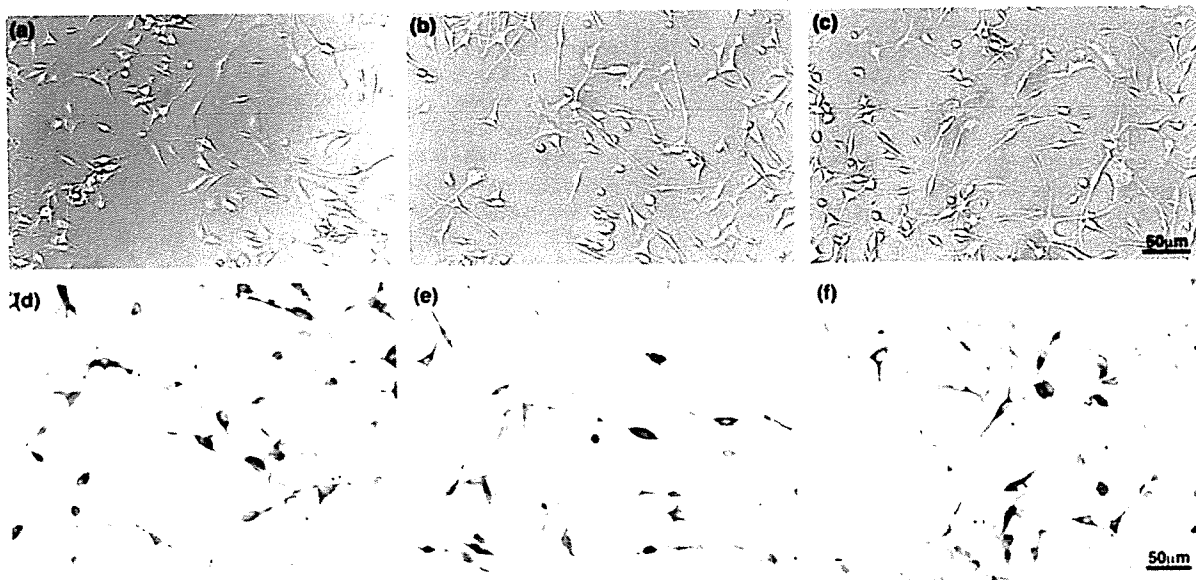
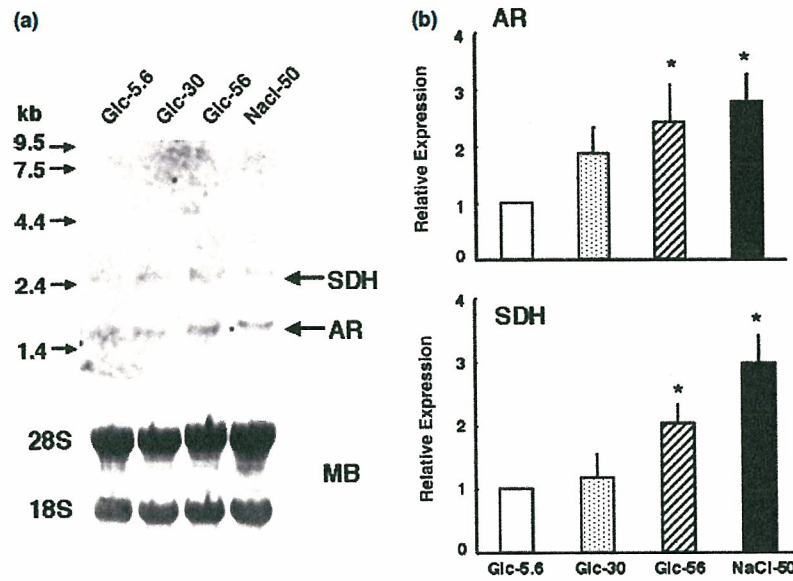


Fig. 1 IMS32 showed distinct Schwann cell phenotypes such as spindle-shaped morphology (a–c) and immunoreactivity to S100 protein (d–f) under normal [Glc-5.6 (a, d)] and high [Glc-30 (b, e) and Glc-56 (c, f)] glucose conditions.



**Fig. 2** Relative mRNA expressions of AR and SDH in IMS32 determined by northern blot analysis. (a) The picture of the blot hybridized with alkaline-phosphatase-labelled cDNA probes (upper panel). Marker molecular masses for calibration are indicated on the left. mRNA for AR and SDH were detected as single bands corresponding to the molecular weight of around 1.4 and 2.4 kb, respectively. The blot showed more intense signals for AR mRNA in Glc-30, Glc-56 and NaCl-50 than that in Glc-5.6, and more intense signals for SDH mRNA

in Glc-56 and NaCl-50 than that in Glc-5.6. A methylene blue-stained image of the duplicate membrane (lower panel) showed that relatively equal amounts of RNA were loaded. (b) The mRNA expressions of AR (upper panel) and SDH (lower panel) in Glc-30, Glc-56 and NaCl-50 relative to those in Glc-5.6. Values represent the mean  $\pm$  SEM of four experiments. \* $p < 0.05$  (by Bonferroni Dunn post-hoc analysis) as compared with Glc-5.6.

2.03 in Glc-56 and 2.99 in NaCl-50; SDH mRNA expression was significantly up-regulated under the high glucose (Glc-56) and hyperosmotic (NaCl-50) conditions.

#### Up-regulated AR protein expression under high glucose and hyperosmotic conditions

By western blot analysis with a polyclonal anti-AR antibody, the expression band of AR was identified as the level of around 36 kDa in molecular size (Fig. 3a, upper). The blot showed more intense signals for AR protein in Glc-30, Glc-56 and NaCl-50 than those in Glc-5.6. There was no significant difference in the signal intensity to  $\beta$ -actin between normal and high glucose/hyperosmotic conditions (Fig. 3a, lower). The average values of relative expression were 1 in Glc-5.6, 1.79 in Glc-30, 2.15 in Glc-56 and 1.95 in NaCl-50, respectively; AR protein expression was up-regulated under the high glucose (Glc-30 and Glc-56) and hyperosmotic (NaCl-50) conditions, although the difference in the values between Glc-30 and Glc-5.6 was not statistically significant. Immunocytochemical analysis revealed the localization of AR protein in the cytoplasm of IMS32. The immunoreactivity for AR was markedly enhanced in Glc-30 (Fig. 4b) compared with Glc-5.6 (Fig. 4a), whereas we saw no significant difference in the immunoreactivity for S100 between the two culture conditions (Fig. 1).

#### Intracellular polyol levels under normal and high glucose conditions

The intracellular contents of sorbitol and fructose were significantly higher in Glc-30 ( $17.9 \pm 1.7$  and  $77.7 \pm 6.7$  nmol/mg) than those in Glc-5.6 ( $1 \pm 0.2$  and  $13.6 \pm 3.4$  nmol/mg; Fig. 5a). The polyol levels in the cells under Glc-56 were extremely high and beyond the range of measurement. The application of an AR inhibitor, SNK-860, to the high glucose (Glc-30) condition for 7 days significantly reduced the polyol contents to levels close to those under normal glucose (Glc-5.6) conditions (i.e. sorbitol  $17.9 \pm 1.7$  nmol/mg in Glc-30 vs.  $3.4 \pm 0.4$  nmol/mg in Glc-30/SNK and fructose  $77.7 \pm 6.7$  nmol/mg in Glc-30 vs.  $29.2 \pm 4.8$  nmol/mg in Glc-30/SNK). The western blot analysis performed in parallel with the measurement of the polyols revealed that the level of AR protein in Glc-30 was not reduced by treatment with SNK-860 (not shown).

#### Gene expression profiles in IMS32 under normal and high glucose conditions

Among nearly 20 000 mouse genes, we identified 28 genes with altered expression in the high glucose (Glc-30) conditions; 10 genes were expressed at a 2.0-fold or greater level, while 18 genes were down-regulated by 2.0-fold or more (Table 1). The relative expression of AR mRNA was 1.2

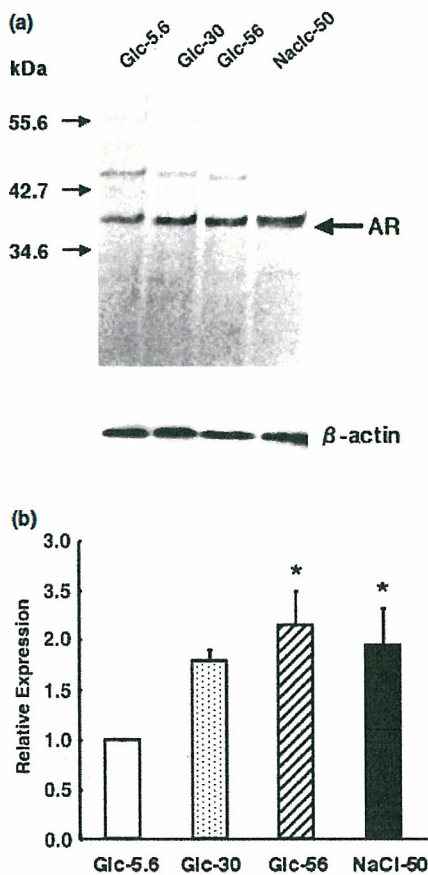


**Fig. 3** Relative protein expression of AR in IMS32 determined by western blot analysis. (a) The picture of the blot incubated with a polyclonal anti-AR antibody (upper panel). Marker molecular masses for calibration are indicated on the left. The expression band of AR was identified as the level a molecular size of around 36 kDa. The blot showed more intense signals for AR protein in Glc-30, Glc-56 and NaCl-50 than that in Glc-5.6. The blot incubated with a monoclonal anti- $\beta$ -actin antibody (lower panel) showed that there was no significant difference in the signal intensity among each experimental group. (b) The protein expression of AR in Glc-30, Glc-56 and NaCl-50 relative to that in Glc-5.6. Values represent the mean + SEM of three experiments. \* $p < 0.05$  as compared with Glc-5.6.

(< 2-fold), and therefore AR was not included in the up-regulated genes in the table. To confirm the microarray results, we measured the relative expression of these genes in the cells under Glc-5.6, Glc-30 and Glc-30/SNK by RT-PCR or northern blot analysis. Thus far, RT-PCR analysis resulted in the significant up-regulation of three genes in Glc-30 compared with Glc-5.6 – SAA3, ANGPTL4 and Evi3 (Fig. 6). Northern blot analysis revealed the down-regulation of mRNA expression for aldehyde reductase (EC 1.1.1.2, aka AKR1A4; Fig. 7). Treatment with SNK-860 had no effects on the mRNA expressions for SAA3, ANGPTL4 or

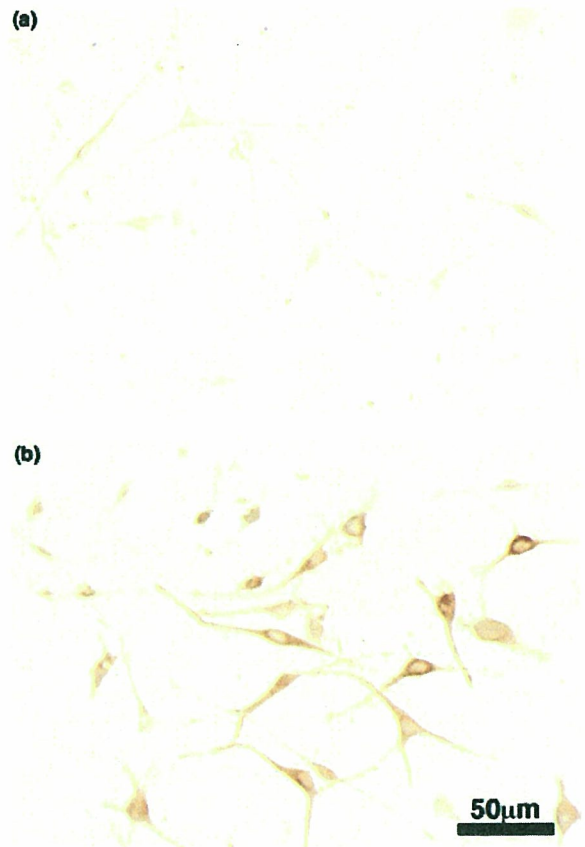


**Fig. 4** Immunocytochemical localization of AR protein in the cytoplasm of IMS32. The photomicrographs showed more intense immunoreactivity for AR in Glc-30 (b) than that in Glc-5.6 (a).

Evi3, but restored the diminished mRNA expression for AKR1A4 to a level equivalent to Glc-5.6 (Figs 6 and 7). These four genes were expressed in the DRG and spinal nerves of adult normal mice, as well as in IMS32 cells (Fig. 8).

## Discussion

### Phenotypic and biochemical features of the Schwann cell line IMS32

IMS32 cells showed distinct Schwann cell phenotypes, such as spindle-shaped morphology and intense immunoreactivity for S100 (Fig. 1), p75<sup>NTR</sup>, laminin and several Schwann cell-specific transcription factors and neurotrophic factors (Watabe *et al.* 1995, 2003). Similar to primary and long-term cultured Schwann cells, IMS32 cells exhibit mitogenic responses to several growth factors [e.g. platelet-derived growth factor BB homodimer (PDGF-BB), acidic and basic fibroblast growth factor (aFGF, bFGF), transforming growth factor (TGF)- $\beta$ 1, 2]. In contrast, IMS32 cells are different

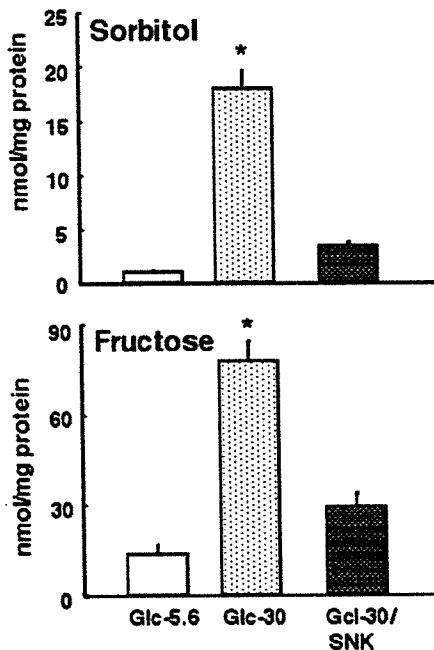


Fig. 5 Intracellular contents of sorbitol (upper panel) and fructose (lower panel) determined by liquid-chromatography. Values expressed as nmol/mg protein represent the mean + SEM of four experiments. \* $p < 0.01$  as compared with Glc-5.6 or Glc-30/SNK.

from primary and long-term cultured Schwann cells in that the former were not contact inhibited and formed ball-shaped subcolonies when cultures reached confluence (Watabe *et al.* 1995). We failed to show that the cell line could myelinate a mouse axon (Watabe *et al.* unpublished observations), in the same way as endogenous Schwann cells in the peripheral nerves and primary cultured Schwann cells (Suzuki *et al.* 1999). In spite of those differences from normal Schwann cells, IMS32 cells have advantages for the study of diabetic neuropathy, such as the activation of the polyol pathway (shown in this study) and the decreased proliferative activity (Kato *et al.* 2003; Nakamura *et al.* 2003) under high glucose conditions mimicking hyperglycaemia *in vivo*.

#### Activation of the polyol pathway in IMS32 under high glucose ( $\geq 30$ mM) environments

In the present study, we observed the significant up-regulation of the mRNA expression for AR and SDH and protein expression for AR under Glc-56 (Figs 2 and 3), and marked increases in the intracellular sorbitol and fructose contents under Glc-30 (Fig. 5) and Glc-56 (beyond the range of measurement), compared with those under Glc-5.6. Although not statistically significant, AR expressions at both mRNA and protein levels under Glc-30 were approximately 1.8-fold higher than those under Glc-5.6. These findings were in line with the enhanced AR immunoreactivity under

Glc-30 according to immunocytochemistry (Fig. 4). We did not measure the enzyme activity in the cells, but the excessive production of sorbitol and fructose under Glc-30 and Glc-56 suggests the high glucose-induced activation of AR and SDH. Furthermore, the application of an AR inhibitor, SNK-860, to Glc-30 for 7 days diminished the intracellular polyol contents to a level close to Glc-5.6. Taking these findings together, the exposure of IMS32 to the high glucose ( $\geq 30$  mM) environments is likely to enhance the expression and activity of AR, thereby leading to exaggerated flux through the polyol pathway. Significant up-regulation of mRNA and protein expressions for AR under Glc-56 and NaCl-50 suggests that AR is induced by not only high glucose but hyperosmotic conditions. The increased expression of AR under hyperosmotic environments has been reported in a variety of cells, and indicates the osmoregulatory role of AR (Yabe-Nishimura 1998). Compared with AR, much less information is available concerning the expression of SDH. The mRNA expression of SDH was not induced by hyperosmolality in rat Schwann cells (Maekawa *et al.* 2001) or renal collecting duct cells (Grunewald *et al.* 1998). Those findings are contrary to the results in this study, i.e. the significant up-regulation of SDH mRNA expression under Glc-56 and NaCl-50. Although the reasons for such variable results among the cells are unknown, we clearly demonstrated that the exposure to high glucose or hyperosmotic environments could induce both AR and SDH mRNA in IMS32.

It remains to be elucidated why an increase in the glucose concentration to 20–30 mM, corresponding to the plasma level in poorly controlled diabetic patients, accelerated the polyol pathway in IMS32, but not in other cultured Schwann cells (Mizisin *et al.* 1996; Suzuki *et al.* 1999; Maekawa *et al.* 2001). In adult rat Schwann cells, neither AR expression/activity nor intracellular sorbitol levels were enhanced under 30-mM glucose conditions. However, the extracellular sorbitol level under those conditions was increased significantly compared with that in the 5.6-mM glucose conditions (Suzuki *et al.* 1999). These findings suggested that sorbitol was released from the cells into the media by an unidentified transport mechanism. In JS1 Schwannoma cells, sorbitol did not accumulate under 25 mM glucose nor 100 mM NaCl conditions unless a SDH inhibitor was applied (Mizisin *et al.* 1997). In contrast with those cells, conspicuous increases of intracellular sorbitol (18-fold) and fructose (6-fold) levels were observed in IMS32 under Glc-30. It seems possible that IMS32 cells possess a much higher capacity than other Schwann cells to store sorbitol and other glucose-derived metabolites. To verify this possibility, we are now investigating if the levels of dicarbonyl intermediates, such as methylglyoxal and 3-deoxyglucosone (Kikuchi *et al.* 1999) in IMS32, are elevated under Glc-30. It is also noteworthy that immortalized Schwann cells were established from not only normal

Table 1 Altered gene expression in IMS32 under the high glucose ([Glc-30]) versus normal glucose ([Glc-5.6]) condition

GenBank Accession No.	Gene	Molecular Function	Ratio ([Glc-30]/[Glc-5.6])
<b>Up-regulated</b>			
AK003182	Myosin light chain, alkali, fast skel.	calcium ion binding (cytoskeleton organization and biogenesis)	2.04
NM_008182	Glutathione S-transferase alpha 2	glutathione transferase activity (detoxification of lipid aldehydes)	2.46
NM_009426	Thyrotropin-releasing hormone (TRH)	thyrotropin-releasing hormone activity	2.04
NM_011315	Serum amyloid A3 (SAA3)	acute-phase response protein activity, lipid transporter activity	2.61
NM_020581	Angiopoietin-like 4 (ANGPTL4)	inhibiting lipoprotein lipase activity, angiogenesis	2.3
NM_023557	RIKEN cDNA 2210409D01	unknown	3.35
NM_144731	UDP-N-acetyl-alpha-D-galactosamine:polypeptide N-acetyl-galactosaminyl transferase (GALNT7)	polypeptide N-acetyl-galactosaminyltransferase activity, transferase activity, transferring glycosyl groups	2.43
NM_144876	RIKEN cDNA D930050H05	unknown	3.21
NM_145492	Ecotropic viral integration site3 (Evi-3)	a retroviral integration site in murine B-cell lymphoma	3.13
NM_146720	Olfactory receptor 421 (Olf421)	olfactory receptor function	2.05
<b>Down-regulated</b>			
AK019076	Adult male tongue cDNA (RAP1 GTPase activating protein 1H)	unknown	0.37
NM_008474	Type II 65kd keratin (KRT-2-16)	structural constituent of cytoskeleton	0.44
NM_007392	Alpha 2 actin	structural constituent of cytoskeleton	0.49
NM_007810	Cytochrome P450, 19, aromatase (Cyp19)	monooxygenase activity, oxidoreductase activity	0.45
NM_008522	Lactoferrin	ferric iron binding	0.43
NM_008826	Phosphofructokinase	6-phosphofructokinase activity (glycolysis)	0.49
NM_009075	Ribose 5-phosphate isomerase	ribose-5-phosphate isomerase activity (pentose-phosphate shunt)	0.44
NM_010266	Guanine deaminase	hydrolase activity	0.43
NM_011144	Peroxisome proliferation activated receptor alpha (PPARα)	transcription factor activity (regulation of fatty acid metabolism)	0.45
NM_013549	Histone2, H2AA1	unknown	0.34
NM_013713	Keratin associated protein 15	unknown (differentiation of epithelial cells?)	0.29
NM_018873	P140 protein	controlling actin cytoskeleton organization	0.42
NM_019467	Allograft inflammation factor 1 (AIF1)	a potential modulator of macrophage activation	0.43
NM_019752	Serine protease (Prss25)	serine-type endopeptidase activity (proteolysis, apoptosis)	0.37
NM_020009	FK506 binding protein associated protein 1 (FRAP1)	inositol/phosphatidylinositol kinase activity	0.27
NM_021473	Abdo-keto reductase (AKR1A4)	aldehyde reductase activity, oxidoreductase activity	0.39
NM_023115	Protocadherin 15 (PCDH15)	calcium ion binding (homophilic cell adhesion)	0.19
NM_024464	RIKEN cDNA 2010319C14	unknown	0.24
NM_025692	RIKEN cDNA 5730525G14	unknown	0.28



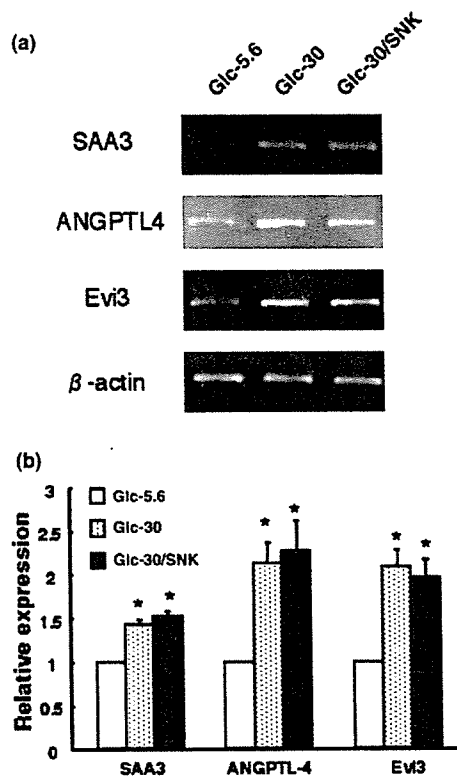


**Fig. 6** Relative mRNA expressions of serum amyloid A3 (SAA3), angiopoietin-like 4 (ANGPTL4) and ecotropic viral integration site 3 (Evi3) in IMS32 determined by semiquantitative RT-PCR. (a) Gel electrophoresis show more intense signals for SAA3, ANGPTL4 and Evi3 mRNA in Glc-30 and Glc-30/SNK than in Glc-5.6. (b) The mRNA expressions of SAA3, ANGPTL4 and Evi3 in Glc-30 and Glc-30/SNK relative to those in Glc-5.6. Values represent the mean + SEM of four experiments. \* $p < 0.05$  as compared with Glc-5.6.

adult mice but also from mouse models of metabolic diseases such as Niemann–Pick disease type C (NPC; *spm/spm*, *npc<sup>nh</sup>/npc<sup>nh</sup>*; Watabe *et al.* 2001, 2003), globoid cell leukodystrophy (twitcher; Shen *et al.* 2002) and  $G_{M2}$  gangliosidosis (Ohsawa *et al.* 2005). The cells originated from those mouse models were able to survive and proliferate in culture, despite the progressive accumulation of undegraded substrates in the cytoplasm.

#### High glucose-induced alterations of gene expression profiles in IMS32

In recent studies, gene expression patterns in DRG (Burnand *et al.* 2004), superior mesenteric and celiac ganglia (SMG-CG) and superior cervical ganglia (SCG) (Carroll *et al.* 2004) were compared between streptozotocin (STZ)-diabetic and control rats via microarray profiling. Those approaches appear to be useful to elucidate the molecular mechanism of the development of diabetic neuropathy. However, the peripheral ganglia contain neurons, Schwann cells and other

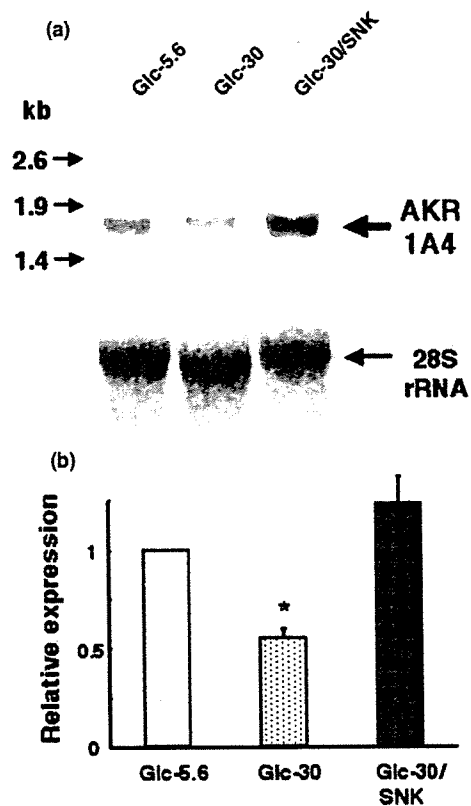


**Fig. 7** Relative mRNA expression of aldehyde reductase (AKR1A4) in IMS32 determined by northern blot analysis. (a) The picture of the blot hybridized with an alkaline-phosphatase-labelled cDNA probe (upper panel). mRNA for AKR1A4 was detected as a single band corresponding to a molecular weight of around 1.7 kb. The blot showed a less intense signal for AKR1A4 mRNA in Glc-30 than that in Glc-5.6 or Glc-30/SNK. A methylene blue-stained image (28S ribosomal RNA) of the duplicate membrane (lower panel) showed that a relatively equal amount of RNA was loaded. (b) The mRNA expression of AKR1A4 in Glc-30 and Glc-30/SNK relative to that in Glc-5.6. Values represent the mean + SEM of four experiments. \* $p < 0.05$  as compared with Glc-5.6 or Glc-30/SNK.

cells, and the microarray studies on them are not sufficient to specify the cells with altered gene expressions. By employing DNA microarray and subsequent RT-PCR or northern blot analyses, we investigated the gene expression profiles in IMS32 exposed to normal (Glc-5.6) and high (Glc-30) glucose conditions. Because 30 mM glucose in culture medium (Glc-30) is closer to the blood glucose concentration in diabetic individuals than 56 mM (Glc-56), we thought that the findings from the comparison between Glc-30 and Glc-5.6 could be more relevant to the *in vivo* studies between diabetic and normal conditions. Although the expression of AR mRNA/protein was not significantly up-regulated by exposure to Glc-30 (Figs 2 and 3, and Table 1), intracellular contents of sorbitol and fructose under

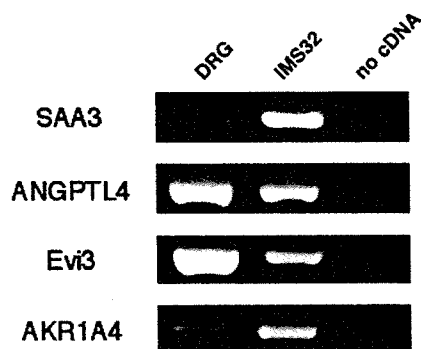


Fig. 8 mRNA expression of SAA3, ANGPTL4, Evi3 and AKR1A4 in the peripheral nerves of an adult mouse: RT-PCR analysis. The pictures of gel electrophoresis showed the PCR products from the cDNA of adult mouse DRG associated with spinal nerve bundles, IMS32 cells, and PCR reactions without a template cDNA, respectively.

Glc-30 were markedly higher than those under Glc-5.6. It seems possible that the degree of increases in the enzyme activity of AR does not correlate with that in the mRNA/protein expression in IMS32 under Glc-30.

The microarray analysis revealed 10 up-regulated genes and 18 down-regulated genes under the high glucose conditions (Table 1). Among the up-regulated molecules, glutathione S-transferase  $\alpha 2$  (GST $\alpha 2$ ) is an isozyme of GST and may be involved in the detoxification of lipid peroxidation products generated by oxidative stress under hyperglycaemic conditions (Srivastava *et al.* 1995; Obrosova 2002). Among the down-regulated genes, phosphofructokinase, one of the key glycolytic enzymes, is essential for the maintenance of axonal integrity; endogenous aldehydes originating from the lipid-peroxidation process are potent inhibitors of this enzyme and may cause significant nerve damage (Novotny *et al.* 1994). Peroxisome proliferator-activated receptor  $\alpha$  (PPAR $\alpha$ ) is an isotype of PPAR, transcription factors involved in the regulation of lipid and glucose metabolism (Staels and Fruchart 2005). Shibata *et al.* (2000) observed that treatment with JTT501, a PPAR $\alpha$  and  $-\gamma$  agonist, prevented the development of diabetic neuropathy in Zucker diabetic fatty rats. However, further RT-PCR/northern blot analyses failed to show the high glucose-induced changes of expression of these genes. In contrast, these analyses confirmed the microarray results, such as significant up-regulation of mRNA expressions for SAA3, ANGPTL4 and Evi3, and the down-regulation of aldehyde reductase (AKR1A4) mRNA expression.

#### SAA3

Serum amyloid A (SAA), a family of apolipoproteins associated with high-density lipoprotein, is known as an

acute-phase reactant (Meek *et al.* 1992). There is an increasing body of evidence that correlates the diabetic conditions with the chronic elevation of SAA (Hamano *et al.* 2004) and the up-regulation of SAA3 (Lin *et al.* 2001), but their significance remains to be elucidated. SAA, as well as advanced glycation end products (AGE), is one of the ligands for the receptor for AGE (RAGE) and the RAGE–ligand interaction is likely to induce cellular dysfunction, thereby being implicated in the development of diabetic complications (Schmidt *et al.* 2000). In addition, Chung *et al.* (2000) observed intense immunoreactivity for SAA in the brains of patients with neurodegenerative diseases such as Alzheimer's disease and multiple sclerosis; the major site of SAA staining in both diseases was the myelin sheaths and axonal membrane. Taking this finding, together with the evidence that SAA can inhibit lipid biosynthesis (Schreiber *et al.* 1999), up-regulation of SAA in nervous tissue under hyperglycaemic conditions might affect myelin lipid synthesis.

#### ANGPTL4

The ANGPTL4 gene is predominantly expressed in the adipose tissue and liver, but its induction in ischaemic tissues (Le Jan *et al.* 2003) implies a role of this molecule in the compensatory angiogenesis for ischaemia and hypoxia (Deindl *et al.* 2001). ANGPTL4 is recognized as a downstream target gene of PPAR $\alpha$  and  $-\gamma$  (Kersten *et al.* 2000), and induces hyperlipidaemia by inhibiting lipoprotein lipase (LPL) activity (Yoshida *et al.* 2002). LPL is expressed in cultured Schwann cells and may play a role in myelin phospholipid biosynthesis in the peripheral nervous system (Huey *et al.* 1998). Ferreira *et al.* (2002) reported that the activity of LPL in the sciatic nerves was reduced in STZ-diabetic rats and restored by treatment with insulin. Taking these findings into consideration, it seems possible that up-regulated ANGPTL4 in Schwann cells under hyperglycaemic conditions inhibits LPL activity, thereby being one of the causes for the impaired fatty acid metabolism and deficient phospholipid synthesis in nervous tissue (Cameron *et al.* 1998; Martin *et al.* 2003). SAA may also play a role in the lipid synthesis as described above, but the interaction between the two molecules remains unknown.

#### Evi3

Evi3 is a common retroviral integration site in murine B-cell lymphoma and encodes a novel zinc finger protein (Warming *et al.* 2003). Because very few papers described this molecule (most of them were focused on tumorigenesis in haematopoietic cells), we currently have no information or idea of how this molecule is involved in the pathobiology of diabetic neuropathy. Treatment with SNK-860 had no effects on the mRNA expressions for SAA3, ANGPTL4 or Evi3 under Glc-30 in this study. This finding suggests that the

up-regulation of these genes in IMS32 under high glucose conditions is not related to the polyol pathway hyperactivity.

#### AKR1A4

Aldehyde reductase is a member of the aldo-keto reductase (AKR) superfamily (the AKR1A subfamily represents the aldehyde reductases and the AKR1B subfamily represents the aldose reductases) (Allan and Lohnes 2000; Hyndman *et al.* 2003). Approximately 50% of the amino acid sequences are conserved between aldehyde reductase and AR (Bohren *et al.* 1989), and both enzymes catalyze the reduction of reactive biogenic aldehydes [e.g. glyceraldehyde, methylglyoxal (MG), hydroxynonenal (HNE) and glucosones] by using NADPH as a cofactor (Flynn 1986; Vander Jagt *et al.* 1992). Unlike AR, aldehyde reductase is virtually inactive for glucose and other aldo sugars (Kawasaki *et al.* 1989). Consequently, much less attention has been paid to aldehyde reductase than AR in the research field of diabetes and its complications (Takahashi *et al.* 1995; Danesh *et al.* 2003). In the present study, reduced mRNA expression of aldehyde reductase in IMS32 under high glucose conditions was completely ameliorated by treatment with an AR inhibitor, SNK-860. The activated AR enhances the flux through the polyol pathway by converting glucose to sorbitol, but it may also act against reactive aldehydes and related substances produced by lipid peroxidation and oxidative stress under hyperglycaemic conditions (Rittner *et al.* 1999; Obrosova 2002). Like AR, aldehyde reductase appears to be able to neutralize lipid peroxidation products (Suzuki *et al.* 1998), but the results in this study suggest that the production of this enzyme is suppressed by augmented expression and activity of AR in Schwann cells during hyperglycaemic conditions. Conversely, AR inhibition may up-regulate aldehyde reductase to be more active against the toxic substances induced by high glucose. This idea is partly supported by findings from previous studies which suggested the functional redundancy of the two enzymes in rat sympathetic ganglia (Kawamura *et al.* 1999, 2002). Moreover, a lack of apparent phenotypes, except a slightly defective urine-concentrating ability in AR-knockout mice (Ho *et al.* 2000), led us to speculate that the detoxification function may be taken over by aldehyde reductase in the absence of AR. However, there has been no direct evidence to indicate such redundancy of these enzymes under hyperglycaemic conditions. It is also important to note that aldehyde dehydrogenase (ALDH) and alcohol dehydrogenase (ADH), as well as AR and aldehyde reductase, can participate in the detoxification of reactive aldehydes in nervous tissue (Picklo *et al.* 2001). A recent report by Suzuki *et al.* (2004) implied the association of the ALDH2/ADH2 polymorphism with the development of human diabetic neuropathy. We expect that further studies focusing on the expression and activity of aldehyde reductase in the peripheral nervous system under hyperglycaemic conditions, espe-

cially in relation to those of AR, ALDH and ADH, will elucidate the role of this enzyme in the pathogenesis of diabetic neuropathy.

The mRNA expression of SAA3, ANGPTL4, Evi3 and AKR1A4 in DRG and spinal nerves in adult normal ICR mice (Fig. 8) suggests their functional roles in the peripheral nervous system. We are about to determine if the expression of these genes is altered in the nerves of STZ-diabetic mice. The antibodies to these proteins are not available from a commercial source, and we plan to collaborate with laboratories studying these molecules. Future studies with the antibodies will help elucidate the immunochemical localization and function of these proteins in the peripheral nervous system and their involvement in the pathogenesis of diabetic neuropathy.

#### Conclusion

The findings in this study indicate the activation of the polyol pathway and the altered gene expression profiles (i.e. up-regulation of SAA3, ANGPTL4 and Evi3 mRNA and down-regulation of AKR1A4 mRNA) in IMS32 under exposure to a high glucose ( $\geq 30$  mM) environment. Considering that an increase in glucose concentration to 20–30 mM accelerated the polyol pathway in IMS32, but not in other previously reported Schwann cells, the culture system of IMS32 under high glucose conditions may provide useful information about the pathogenesis of diabetic neuropathy, especially polyol pathway-related abnormalities.

#### Acknowledgements

This work was supported by a Grant-in-aid for Scientific Research from the Japanese Ministry of Education, Science, Sports and Culture, and grants from the Sanwa Kagaku Kenkyusho, Suzuken Memorial Foundation and the Japan Diabetes Foundation. We thank Drs Hitoshi Kawano, Koichi Kato, Noriaki Kato and Miwa Sango-Hirade for the helpful suggestions, and Akiko Tokashiki and Kyoko Ajiki for their technical assistance.

#### References

- Allan D. and Lohnes D. (2000) Cloning and developmental expression of mouse aldehyde reductase (AKR1A4). *Mech. Dev.* **94**, 271–275.
- Bohren K. M., Bullock B., Wermuth B. and Gabbay K. H. (1989) The aldo-keto reductase superfamily. cDNAs and deduced amino acid sequences of human aldehyde and aldose reductases. *J. Biol. Chem.* **264**, 9547–9551.
- Burnand R. C., Price S. A., McElhaney M., Barker D. and Tomlinson D. R. (2004) Expression of axotomy-inducible and apoptosis-related genes in sensory nerves of rats with experimental diabetes. *Brain Res. Mol. Brain Res.* **132**, 235–240.
- Cameron N. E., Cotter M. A., Horrobin D. H. and Tritschler H. J. (1998) Effects of  $\alpha$ -lipoic acid on neurovascular function in diabetic rats: interaction with essential fatty acids. *Diabetologia* **41**, 390–399.
- Carroll S. L., Byer S. J., Dorsey D. A., Watson M. A. and Schmidt R. E. (2004) Ganglion-specific patterns of diabetes-modulated gene

- expression are established in prevertebral and paravertebral sympathetic ganglia prior to the development of neuroaxonal dystrophy. *J. Neuropathol. Exp. Neurol.* **63**, 1144–1154.
- Chung T. F., Sipe J. D., McKee A., Fine R. E., Schreiber B. M., Liang J. S. and Johnson R. J. (2000) Serum amyloid A in Alzheimer's disease brain is predominantly localized to myelin sheaths and axonal membrane. *Amyloid* **7**, 105–110.
- Danesh F. R., Wada J., Walner E. I., Sahai A., Srivastava S. K. and Kanwar Y. S. (2003) Gene regulation of aldose-, aldehyde- and renal specific oxido reductase (RSOR) in the pathobiology of diabetes mellitus. *Curr. Med. Chem.* **10**, 1399–1406.
- Deindl E., Buschmann I., Hoefler I. E., Podzuweit T., Boengler K., Vogel S., van Royen N., Fernandez B. and Schaper W. (2001) Role of ischemia and of hypoxia-inducible genes in arteriogenesis after femoral artery occlusion in the rabbit. *Circ. Res.* **89**, 779–786.
- Dyck P. J. and Giannini C. (1996) Pathologic alterations in the diabetic neuropathies of humans: a review. *J. Neuropathol. Exp. Neurol.* **55**, 1181–1193.
- Eckersley L. (2002) Role of the Schwann cell in diabetic neuropathy. *Int. Rev. Neurobiol.* **50**, 293–321.
- Ferreira L. D., Huey P. U., Pulford B. E., Ishii D. N. and Eckel R. H. (2002) Sciatic nerve lipoprotein lipase is reduced in streptozotocin-induced diabetes and corrected by insulin. *Endocrinology* **143**, 1213–1217.
- Flynn T. G. (1986) Aldose and aldehyde reductase in animal tissues. *Metabolism* **35**, 105–108.
- Grunewald R. W., Wagner M., Schubert I., Franz H. E., Muller G. A. and Steffgen J. (1998) Rat renal expression of mRNA coding for aldose reductase and sorbitol dehydrogenase and its osmotic regulation in inner medullary collecting duct cells. *Cell Physiol. Biochem.* **8**, 293–303.
- Guerrant G. and Moss C. W. (1984) Determination of monosaccharides as aldononitrile, *O*-methoxime, alditol, and cyclitol acetate derivatives by gas chromatography. *Anal. Chem.* **56**, 633–638.
- Gui T., Tanimoto T., Kokai Y. and Nishimura C. (1995) Presence of a closely related subgroup in the aldo-keto reductase family of the mouse. *Eur. J. Biochem.* **227**, 448–453.
- Hamano M., Saito M., Eto M., Nishimatsu S., Suda H., Matsuda M., Matsuki M., Yamamoto S. and Kaku K. (2004) Serum amyloid A, C-reactive protein and remnant-like lipoprotein particle cholesterol in type 2 diabetic patients with coronary heart disease. *Ann. Clin. Biochem.* **41**, 125–129.
- Ho H. T., Chung S. K., Law J. W., Ko B. C., Tam S. C., Brooks H. L., Knepper M. A. and Chung S. S. (2000) Aldose reductase-deficient mice develop nephrogenic diabetes insipidus. *Mol. Cell Biol.* **20**, 5840–5846.
- Huey P. U., Marcell T., Owens G. C., Etienne J. and Eckel R. H. (1998) Lipoprotein lipase is expressed in cultured Schwann cells and functions in lipid synthesis and utilization. *J. Lipid Res.* **39**, 2135–2142.
- Hyndman D., Bauman D. R., Heredia V. V. and Perming T. M. (2003) The aldo-keto reductase superfamily homepage. *Chem. Biol. Interact.* **143–144**, 621–631.
- Kato K., Nakamura J., Kamiya H. *et al.* (2003) Effect of high glucose and C-peptide on proliferation and MAP kinase activity in cultured immortalized mouse Schwann (IMS32) cells. *J. Peripher. Nerv. Syst. (Abstr.)* **8**, 183.
- Kawamura M., Eisenhofer G., Kopin I. J. *et al.* (1999) Aldose reductase, a key enzyme in the oxidative deamination of norepinephrine in rats. *Biochem. Pharmacol.* **58**, 517–524.
- Kawamura M., Eisenhofer G., Kopin I. J., Kador P. F., Lee Y. S., Fujisawa S. and Sato S. (2002) Aldose reductase: an aldehyde scavenging enzyme in the intraneuronal metabolism of norepinephrine in human sympathetic ganglia. *Auton. Neurosci.* **96**, 131–139.
- Kawasaki N., Tanimoto T. and Tanaka A. (1989) Characterization of aldose reductase and aldehyde reductase from rat testis. *Biochim. Biophys. Acta* **996**, 30–36.
- Kern T. S. and Engelman R. L. (1982) Immunohistochemical distribution of aldose reductase. *Histochem. J.* **14**, 507–515.
- Kersten S., Mandard S., Tan N. S., Escher P., Metzger D., Chambon P., Gonzalez F. J., Desvergne B. and Wahli W. (2000) Characterization of the fasting-induced adipose factor FIAF, a novel peroxisome proliferator-activated receptor target gene. *J. Biol. Chem.* **275**, 28 488–28 493.
- Kikuchi S., Shimpo K., Moriwaka F., Makita Z., Miyata T. and Tashiro K. (1999) Neurotoxicity of methylglyoxal and 3-deoxyglucosone on cultured cortical neurons: synergism between glycation and oxidative stress, possibly involved in neurodegenerative diseases. *J. Neurosci. Res.* **57**, 280–289.
- Le Jan S., Amy C., Cazes A. *et al.* (2003) Angiotensin-like 4 is a proangiogenic factor produced during ischemia and in conventional renal cell carcinoma. *Am. J. Pathol.* **162**, 1521–1528.
- Lee F. K., Lee A. Y. W., Lin C. X. F. *et al.* (1995) Cloning, sequencing, and determination of the sites of expression of mouse sorbitol dehydrogenase cDNA. *Eur. J. Biochem.* **230**, 1059–1065.
- Lin Y., Rajala M. W., Berger J. P., Moller D. E., Barzilai N. and Scherer P. E. (2001) Hyperglycemia-induced production of acute phase reactants in adipose tissue. *J. Biol. Chem.* **276**, 42 077–42 083.
- Low P. A., Nickander K. K. and Scionti L. (1999) Role of hypoxia, oxidative stress, and excitatory neurotoxins in diabetic polyneuropathy, in *Diabetic Neuropathy* (Dyck, P. J. and Thomas, P. K., eds), pp. 317–329. W. B. Saunders, Philadelphia.
- Maekawa K., Tanimoto T., Okada S., Suzuki T., Suzuki T. and Yabe-Nishimura C. (2001) Expression of aldose reductase and sorbitol dehydrogenase genes in Schwann cells isolated from rat: effects of high glucose and osmotic stress. *Brain Res. Mol. Brain Res.* **87**, 251–256.
- Martin A., Komada M. R. and Sane D. C. (2003) Abnormal angiogenesis in diabetes mellitus. *Med. Res. Rev.* **23**, 117–145.
- Meek R. L., Eriksen N. and Benditt E. P. (1992) Murine serum amyloid A3 is a high-density apolipoprotein and is secreted by macrophages. *Proc. Natl Acad. Sci. USA* **89**, 7949–7952.
- Mizisin A. P. and Powell H. C. (2003) Pathogenesis and pathology of diabetic neuropathy, in *Textbook of Diabetic Neuropathy* (Gries, F. A., Cameron, N. E., Low, P. A. and Ziegler, D., eds), pp. 83–169. Georg Thieme Verlag, New York.
- Mizisin A. P., Li L., Perello M., Freshwater J. D., Kalichman M. W., Roux L. and Calcutt N. A. (1996) Polyol pathway and osmotic regulation in JS1 Schwann cells grown in hyperglycemic and hyperosmotic conditions. *Am. J. Physiol.* **270**, F90–F97.
- Mizisin A. P., Li L. and Calcutt N. A. (1997) Sorbitol accumulation and transmembrane efflux in osmotically stressed JS1 schwannoma cells. *Neurosci. Lett.* **229**, 53–56.
- Nakamura J., Kamiya H., Nakae M., Naruse K., Hamada Y., Kato K. and Hotta N. (2003) Effect of bFGF on Schwann cell growth and diabetic neuropathy in rats. *J. Peripher. Nerv. Syst. (Abstr.)* **8**, 188–189.
- Novotny M. V., Yancey M. F., Stuart R., Wiesler D. and Peterson R. G. (1994) Inhibition of glycolytic enzymes by endogenous aldehydes: a possible relation to diabetic neuropathies. *Biochem. Biophys. Acta.* **1226**, 145–150.
- Obrosova I. G. (2002) How does glucose generate oxidative stress in peripheral nerve? *Int. Rev. Neurobiol.* **50**, 3–35.
- Ohsawa M., Kotani M., Tajima Y. *et al.* (2005) Establishment of immortalized Schwann cells from a Sandhoff mouse and corrective effect of recombinant human  $\beta$ -hexosaminidase A on the accumulated GM2 ganglioside. *J. Hum. Genet.* **50**, 460–467.